

Forecast-informed hydropower optimization at long and short-time scales for a multiple dam network

Cite as: J. Renewable Sustainable Energy **12**, 000000 (2020); doi: 10.1063/1.5124097

Submitted: 11 August 2019 · Accepted: 31 January 2020 ·

Published Online: 0 Month 0000



Shahryar Khaliq Ahmad and Faisal Hossain^{a)}

AFFILIATIONS

Department of Civil and Environmental Engineering, University of Washington, More Hall 201, Seattle, Washington 98195, USA

^{a)} Author to whom correspondence should be addressed: fhossain@uw.edu. Tel.: (931) 239- 4665

ABSTRACT

This study presents a scheme for co-optimizing the long-term (seasonal) reservoir operating objectives with the short-term (daily) objectives for multi-dam networks to maximize hydropower generation. Long-term optimal reservoir storage provides temporal space to optimize operation of the dams at short-term based on forecasted reservoir inflow. This study asks if there is an added benefit of co-optimization of operations at long- and short-term scales for hydropower generation. The multi-objective optimization problem at both the temporal scales was simultaneously solved considering Pareto optimality between conflicting objectives. Constraints pertaining to flood control, dam safety, and environmental flow were imposed. The proposed scheme was implemented over a network of Blue Mesa, Morrow Point, and Crystal dams in the Upper Colorado Basin. Ensemble forecast forcings from publicly available numerical weather prediction and climate models were used as inputs for the daily and monthly scale inflow forecasts. The results show improvements of 41%, 27%, and 15% in hydropower generation using the co-optimization during wet, moderate, and dry years, respectively, against a benchmark that neglects inflow forecasts. This study demonstrates added benefit of co-optimizing the operations for hydropower generation based on short- and long-term forecasted reservoir inflow. Given that most dams today operate as a network in a river basin, we recommend moving away from single dam and single time scale optimization to a multiple-dam with long- and short-term scale co-optimization-based operations to make renewable energy generation more efficient.

Published under license by AIP Publishing. <https://doi.org/10.1063/1.5124097>

I. INTRODUCTION

One of the least expensive and stable sources of energy with significant operational flexibility and instant power generation capability is conventional hydropower (Holmes and Papay, 2011). Hydropower has experienced comparatively fewer periods of fluctuations in yield, unlike wind or solar, which are dependent on geographic location and ambient weather conditions (DOE, 2016). To reduce the dependence on fossil fuels and promote the use of clean and renewable energy sources, the operations of hydropower dams (used here interchangeably with “reservoirs”) need to play a critical and central role. Hydropower dams that already exist are not getting phased out globally anytime soon despite the well-known costs to the environment and ecosystem services (Ligon et al., 1995; Tilt et al., 2009). Thus, efficiently managing such a resource has the potential to not only expand clean (i.e., non-fossil fuel) energy generation but also provide resilience against extreme hydrological events, drought management, and flood protection (Yang et al., 2017). As the growing population’s demand

for water and the resulting water stress continues to increase, building newer dam infrastructure is not a fool-proof solution and is much debated in the literature (Manyari and de Carvalho, Jr., 2007; Tilt et al., 2009). Rather, if the existing dams are operated more efficiently, higher energy benefits can be achieved without building new hydropower dams. In other words, improved performance of hydropower operations can generate more energy from fewer dams, while providing the planned hydropower systems with smarter expansion plans (Marques and Tilmant, 2013).

Researchers and policy makers, over the past century, have been attempting to improve the reservoir operations to better satisfy the demands of stakeholders. A major challenge toward improving the operational effectiveness of reservoirs is to integrate the forecast of weather and climate information with real-time operating policies (Dong et al., 2006). A distinction is generally made concerning the temporal scale of forecasts where short-term forecasts (daily to weekly scale) are incorporated to optimize for short-term (tactical) operational

61 purposes while medium to long-term forecasts (monthly or seasonal
 62 scale) are used for long-term (strategic) objectives (Anghileri *et al.*,
 63 2016). Although this is a common notion for using forecast informa-
 64 tion to optimize reservoir operations, it suffers from drawbacks. Losses
 65 can occur to the specified operating purpose due to optimization
 66 addressing only the short or long-term objectives but not both
 67 (Sreekanth *et al.*, 2012). Real-time operations typically rely on forecasts
 68 with a horizon of only a few days because of degrading skill in forecasts
 69 with the increasing lead time (Celeste *et al.*, 2008). However, relying
 70 only on the short-term forecasts for reservoir operation optimization
 71 results in a short-sighted policy that does not dovetail the longer-term
 72 goals. Such release decisions optimal over short-term are prone to
 73 sub-optimality when the performance is assessed over the seasonal or
 74 annual scale (Xu *et al.*, 2015; Sreekanth *et al.*, 2012). Likewise, when the
 75 optimization problem addresses only the long-term planning of the res-
 76ervoir operations, it uses seasonal hydro-climatic information that can
 77 introduce large inflow uncertainty at shorter time scales. Bias in long-
 78 term forecasts of inflow and conflicts between long and short-term
 79 operation goals can again lead to a suboptimal policy over the long-
 80 term as well as over episodic extreme events (Xu *et al.*, 2015).
 81 Therefore, it is imperative now to achieve a balance between the imme-
 82 diate and potential future benefits, satisfying both the short and long-
 83 term optimality in operations. Large dams that operate as a network
 84 can optimize their monthly storage and release based on seasonal
 85 (long-term) forecast of inflow. Such long-term optimization provides
 86 temporal solution space to optimize and tailor the operations of the
 87 dams at short-term (daily) scales based on reservoir inflow using
 88 weather-forecasts. We demonstrate this concept schematically in Fig. 1.
 89 Dams are seldom operated individually and are usually con-
 90 nected in a network, often to form a multi-reservoir system with a cas-
 91 cade of reservoirs in series and occasionally in parallel. Operating the
 92 entire system in coordination with each dam is essential for improving
 93 the operational efficiency and maximizing the overall benefits to the
 94 stakeholder with conflicting interest (Xu *et al.*, 2015). Joint operation
 95 considers the storage variation in each linked reservoir and

subsequently results in a set of optimal releases with simultaneous
 evaluation of numerous trade-offs in the best interest of each reservoir.
 Operating rule curves are often used to guide the operations of system
 of dams outlining the reservoir storage targets to be met at specific
 times of the year. The rules are historically developed by respective
 operating agencies using historical reservoir inflows, physical con-
 straints (e.g., downstream channel capacity), and historical operating
 objectives (Anghileri *et al.*, 2016). A number of reservoir planning and
 operation studies have optimized the rules based on the operating pur-
 pose and type of reservoir network. Lund and Guzman (1999)
 reviewed a variety of derived real-time operating policies for multiple
 reservoir networks operated for water supply, flood control, hydro-
 power, water quality, and recreation and presented conceptual optimal
 rules for series and parallel reservoir networks. Marques and Tilmant
 (2013) underscored the economic value of coordination in a large-
 scale multi-reservoir system in Brazil. Zhou *et al.* (2016) derived
 optimal operating rules for a multi-reservoir system in China by com-
 bining the water and power operating rules to coordinate operations.
 However, most of these published rules are static “thumb rules” that
 cannot be relied upon when the circumstances change. For example,
 during extreme events of unprecedented magnitude, relying upon
 such rules does not guarantee the best degree of resilience or down-
 stream safety. This necessitates a scheme of operations, which is
 dynamically updated at shorter timescales and adjusts itself accord-
 ingly without the need to refer to static rules.

The dimensionality problem in optimizing larger systems is tack-
 led using the aggregation of multiple reservoirs to convert into an
 equivalent single-reservoir optimization problem (Liu *et al.*, 2011).
 This is then followed by a disaggregation scheme to obtain solutions
 for single reservoirs (Saad *et al.*, 1994). Fang *et al.* (2014) proposed the
 hedging rule based on an aggregated reservoir and the storage alloca-
 tion rule to specify release from each reservoir. Archibald *et al.* (1997)
 included a two-dimensional representation of the rest of the system to
 the equivalent aggregated reservoir. Another commonly applied
 approach is to optimize the released and stored energy instead of the

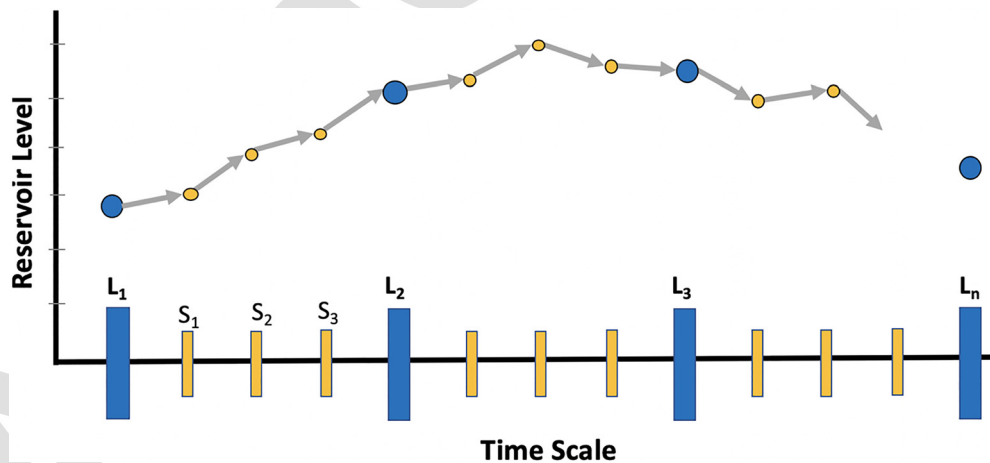


FIG. 1. Schematic showing the concept of co-optimization where the long-term optimal goals are dovetailed with the short-term optimal reservoir operations. Blue bars (L_1, \dots, L_n) are long-term forecast horizon units (or lead times) for obtaining storages optimized for long-term benefits, while yellow bars (S_1, \dots, S_n) denote the short-term optimization horizon. The corresponding short-term optimal operations (gray arrows) result in the levels (yellow circles) that are also optimal with the long-term goals (blue circles). The co-optimization uses temporal solution space to tailor the short-term operating policy within the long-term horizon.

131 objective or cost function. For example, [Becker and Yeh \(1974\)](#) and [Li](#)
132 [et al. \(2012\)](#) proposed the optimal operation model that minimized
133 the loss of released or stored energy. Furthermore, a general rule for
134 increasing hydropower is to prioritize storage in reservoirs with the
135 highest energy production ([Marques and Tilmant, 2013](#)). However,
136 such an approach is biased as the most “efficient” reservoir that needs
137 the least amount of release per unit energy generated always gets more
138 load, leading to faster storage depletion and reducing its productivity
139 ([Xu et al., 2015](#)).

140 A vast majority of literature on deriving optimal operation rules
141 has paid attention to either short-term or long-term forecast-based
142 optimization. The value of long-term inflow forecasts (monthly to sea-
143 sonal scale) has been demonstrated for flood control operations
144 ([Anghileri et al., 2016](#)), hydropower operations ([Hamlet et al., 2002](#);
145 [Block, 2011](#); [Maurer and Lettenmaier, 2004](#); [Alemu et al., 2011](#)), irriga-
146 tion and water supply ([Sankarasubramanian, 2009](#); [Georgakakos et al.,](#)
147 [2005](#)), and drought management ([Golembesky et al., 2009](#)). On the
148 other hand, a few of the studies on short-term (daily to weekly) fore-
149 casts, specifically for hydropower maximization, include [Ahmad et al.](#)
150 [\(2020\)](#), [Monteiro et al. \(2013\)](#), [Madsen et al. \(2009\)](#), and [Fan et al.](#)
151 [\(2016\)](#). There are only a handful of studies that have focused on inte-
152 grating the long-term optimization module with the short-term (daily)
153 operations as a co-optimization strategy.

154 One of the first efforts to integrate the optimization models at dif-
155 ferent temporal scales was proposed by [Becker et al. \(1976\)](#) and [Yeh](#)
156 [\(1979\)](#) for the operation of the California Central Valley Project. The
157 procedure optimizes a monthly model over one year and uses the
158 monthly ending storages into a daily model followed by using the daily
159 releases into an hourly model. [Georgakakos \(2006\)](#) used a similar con-
160 cept for developing the multilayer operation model for Nile Basin.
161 [Dong et al. \(2006\)](#) assessed the effect of flow forecasting quality on the
162 benefits of single-reservoir operation. The ending monthly storage
163 from a long-term optimization model was input as constraints to the
164 short-term daily model. However, the long-term model uses the
165 monthly average of the observed flow series, which results in a single
166 static long-term policy and is not updated as the optimization pro-
167 gresses in time. Also, different levels of noise were added synthetically
168 to the observed inflow to obtain the short-term forecasts. Synthetic
169 forecasts render the optimization results sensitive to the added noise,
170 which are not representative of the actual value in the concept when it
171 is operationalized. [Celeste et al. \(2008\)](#) integrated daily and monthly
172 optimization models over a single reservoir operated for water supply.
173 A deficit term was obtained from the long-term release policy repre-
174 senting how well the demands are met so as to trigger hedging during
175 the short-term operations. This approach does not guide the short-
176 term policy at each time step of the optimization horizon; rather, the
177 operations are only affected when the deficit exceeds a certain thresh-
178 old. [Sreekanth et al. \(2012\)](#) generated synthetic forecast flows to dem-
179 onstrate the nesting of long-term optimization with the short-term
180 model at a time step of five days over a single reservoir in South India.
181 Simple linear constraints were used for using the information from the
182 long-term model into the short-term optimization procedure. [Xu et al.](#)
183 [\(2015\)](#) established a short-term operation model first to minimize the
184 operation cost, and then the non-dominated set of solutions was used
185 as input to a long-term model to select the best strategy for both the
186 temporal scales. Again, historical inflows were used to represent the
187 possible flow scenarios to occur in the future.

Given the history of multi-reservoir optimization, there still 188
remain a few gaps that necessitate attention from the scientific 189
community: 190

- (a) there are hardly any studies that integrate the short and long- 191
term operating objectives simultaneously as a co- 192
optimization problem while updating the optimal policies at 193
both time scales for a multi-reservoir system, specifically for 194
hydropower operations; 195
- (b) the existing studies on co-optimization at the two timescales 196
have only used synthetically generated forecasts by adding 197
noise to the observed inflow time series, which does not rep- 198
resent the true value in such a concept when applied opera- 199
tionally; and 200
- (c) although there have been efforts to study the effect of the 201
quality of flow forecasts on the resulting optimal policy, no 202
comprehensive framework has been developed to assess the 203
added value in co-optimization of the operating policy at 204
short and long-term scales against a conventional baseline 205
with no optimization for multiple dam networks. 206

To address these unresolved issues for hydropower generation in 207
the context of renewable energy sustainability, the present study uses a 208
real-time weather forecasting model at short-term (daily) and a sea- 209
sonal climatic model at long-term (monthly) temporal scales to obtain 210
flow forecasts for the co-optimization model. 211

The specific research questions addressed here are (1) what is the 212
added value of co-optimization in time and space dimension over a 213
multi-dam network operated for hydropower operations? (2) How 214
sensitive is the optimal reservoir operating policy to the skill in short 215
and long-term flow forecasts? 216

The rest of this paper is organized as follows. In Sec. II, the 217
selected site and necessary datasets for the application of the proposed 218
technique are described. This is then followed by a detailed description 219
of the forecasting and reservoir operation optimization model as well 220
as the evaluation framework in Sec. III. The case study results of the 221
application of short- and long-term forecasts for optimization using 222
different strategies for evaluation are presented in Sec. IV. A sensitivity 223
analysis of the skill of long-term forecasts is also included, followed by 224
discussion and concluding remarks in Sec. V. 225

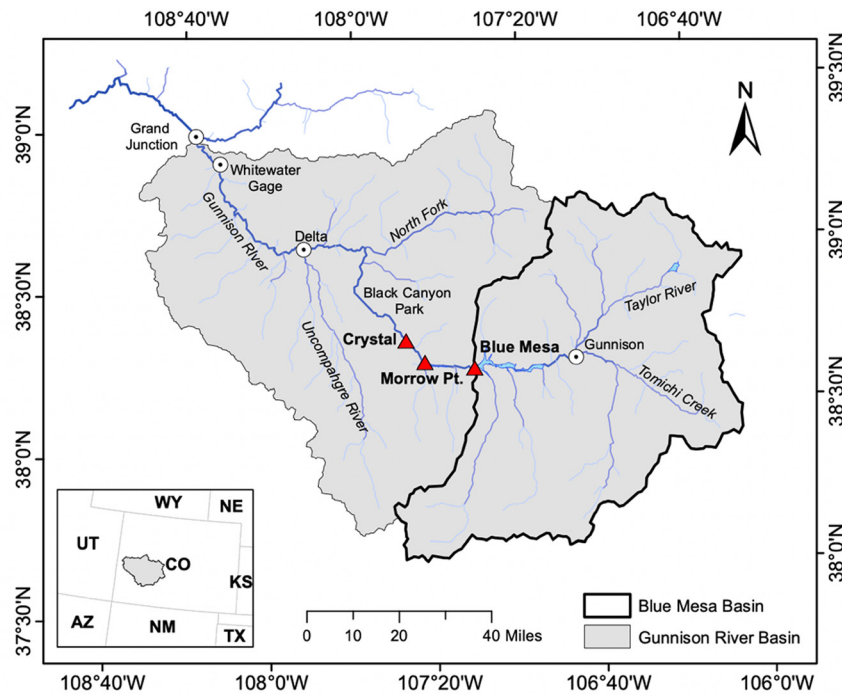
II. STUDY SITE AND DATASETS 226

A. Multi-dam network and its operations 227

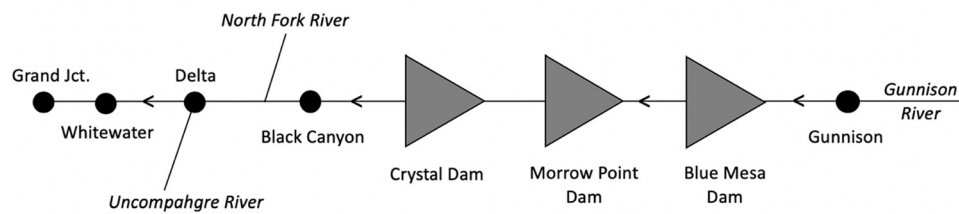
The dam network chosen for the demonstration of the pro- 228
posed technique is one of the four units of the Colorado River 229
Storage Project called Wayne N. Aspinall Unit. The unit is com- 230
posed of a series of three dams—Blue Mesa (BM) Dam, Morrow 231
Point (MP) Dam, and Crystal (CR) Dam in the Upper Colorado 232
Basin along the Gunnison River, which flows further down into the 233
Colorado River. The dams were constructed between 1963 and 1977 234
and are operated by the U.S. Bureau of Reclamation (USBR). A sche- 235
matic of the reservoir connections and relevant hydrological stations 236
is shown in [Fig. 2 \(USBR, 2004\)](#). The drainage basin of the Blue 237
Mesa dam used for reservoir inflow modeling is also shown. [Table I](#) 238
summarizes the characteristics of dams and power plants in the 239
Unit. 240

The upstream-most and largest reservoir, Blue Mesa, is responsi- 241
ble for the primary water storage in the system. The power plants at 242

AQ2



(a)



(b)

FIG. 2. (a) Dams in the Aspinall Unit, pertinent hydrological stations, Gunnison River, and Blue Mesa drainage basins; (b) simplified schematic showing the dam connections and relevant stations (not to scale). Arrows show the flow direction (upstream to downstream).

243 Blue Mesa and Morrow Point are highly flexible with the release rates
 244 and can be operated to provide peaking power. The five turbines at the
 245 three dams are capable of generating up to 291 MW of electricity.
 246 The power plant at the Morrow Point produces the largest amount
 247 of energy, around twice as much as Blue Mesa. The crystal reservoir
 248 serves as a regulation reservoir to stabilize flows to the
 249 Gunnison River and is usually operated under constraints to regulate
 250 downstream flows. The dam releases can be made via power-
 251 houses/penstocks, bypass, or spillway routes. The USBR manages
 252 the releases within certain sideboards that include annual snow-
 253 pack conditions, senior water rights, minimum downstream flow
 254 requirements, power plant and outlet capacities, reservoir elevation
 255 goals, fishery management recommendations, dam safety, and
 256 other considerations. Certain operational goals are mandated to
 257 honor these sideboards, which were used to design constraints for

the optimization model. These goals include but are not limited to 258
 the following (see Fig. 2 for hydrological stations): 259

- (a) the desired Whitewater gage peak flow (USGS station 260
 09152500) to be obtained every year based on the April–July 261
 forecasted inflow into the Blue Mesa reservoir; 262
- (b) flow at the Gunnison River above the confluence with the 263
 Uncompahgre River to be kept below 15 000 cfs; 264
- (c) peak releases be typically made between May 10th and June 1st, 265
 giving priority to power plants followed by bypasses and spillways; 266
- (d) Blue Mesa Reservoir to be kept at or below 7490 feet (580 000 267
 acre-feet live storage) by December 31st to provide storage 268
 for next spring’s runoff and minimize upstream icing; 269
- (e) minimum downstream flow through the Black Canyon of the 270
 Gunnison National Park and Gunnison Gorge National 271

TABLE I. Relevant characteristics of the dams, reservoirs, and power plants in the Aspinall Unit.

Dam, reservoir, and power plant characteristics	Blue Mesa	Morrow point	Crystal
Dam type	Earthfill embankment	Double-curvature thin-arch	Double-curvature thin-arch
Dam height (ft)	502.0	468.0	323.0
Spillway crest elevation ^a (ft)	7487.9	7123.0	6756.0
Crest elevation ^a (ft)	7528.0	7165.0	6772.0
Total storage capacity (acre-ft)	940 700	117 190	25 240
Total installed capacity (MW)	86.4	173.3	32.0
Production mode	Peaking	Peaking	Base load
Number of turbines	2	2	1
Turbine flow capacity (cfs)	3400	5400	2150
Bypass capacity (cfs)	4500	1500	1900
Spillway capacity (cfs)	34 000	41 000	41 350

^aAbove the mean sea level.

272 Conservation Area is 300 cfs, except in severe drought when
 273 flow may be reduced;
 274 (f) maximum releases from the Crystal Dam, outside of the peak
 275 flow period, be limited to the 2150 cfs power plant capacity; and
 276 (g) daily ramping rates at the Crystal Dam limited to the increase
 277 in 500 acre-ft and the decrease of 400 acre-ft per day.

278 **B. Operational and hydrometeorological data**

279 The observed operational data for the Aspinall Unit were
 280 obtained from the USBR's data portal ([https://www.usbr.gov/](https://www.usbr.gov/rsvrWater/HistoricalApp.html)
 281 [rsvrWater/HistoricalApp.html](https://www.usbr.gov/rsvrWater/HistoricalApp.html); [Aspinall Unit Water Operations,](#)
 282 [2019](#)), which include observed inflows, releases, reservoir elevation,
 283 storage, and hydropower generated. The operational data were used
 284 for setting up the optimization model as well as in calibration and vali-
 285 dation of the forecasting models. The hydro-meteorological forecast
 286 forcings, basin's antecedent conditions, and current reservoir state
 287 (from USBR) were inputs to the inflow forecasting model. The forecast
 288 fields of precipitation, temperature, and windspeed were acquired
 289 from the Global Forecast System (GFS) global-scale numerical weather
 290 prediction (NWP) model at 0.5° for a lead time of 7 days with a 3-h
 291 temporal resolution. To include the uncertainty estimates in the fore-
 292 cast flow, National Oceanic and Atmospheric Administration's
 293 (NOAAs) Global Ensemble Forecasting System Reforecast (version 2)
 294 dataset (GEFS/R) ([Hamill et al., 2013](#)) with an 11-member ensemble
 295 of forecasts at 1° resolution was used. The average scenario of the
 296 ensemble members was used for optimizing the reservoir operations.
 297 The antecedent basin precipitation was obtained from the Climate
 298 Hazards Group InfraRed Precipitation with Station data (CHIRPS)
 299 gridded rainfall time series at a resolution of 0.05° ([Funk et al., 2015](#)).
 300 The gridded datasets were converted into basin-averaged estimates for
 301 inputs to the forecasting model.

302 For the monthly scale long-term forecasting model, in addition
 303 to the antecedent monthly streamflow, the ensemble seasonal forecast
 304 forcings from the climate model suite of North American Multi-
 305 Model Ensemble (NMME) were used ([Kirtman et al., 2014](#)). The
 306 diversity of models in NMME provides a superior representation of
 307 multi-model uncertainty in seasonal forecast skill, on average, relative

to other seasonal prediction systems. Because it is computationally 308
 challenging to use each of the ensemble models present in the NMME 309
 suite for optimization, two models were chosen to obtain enough 310
 ensemble members that are representative of the uncertainty in mod- 311
 eled forcings. These were (i) Climate Forecast System version 2 312
 (CFSv2) for monthly precipitation fields ([Saha et al., 2014](#)) and (ii) 313
 Geophysical Fluid Dynamics Laboratory (GFDL) CM2.1 model for 314
 sea surface temperature fields ([Delworth et al., 2006](#)). An additional 315
 predictor of the SST anomaly based index of Niño 3.4 was also used 316
 for the monthly forecast model, retrieved from the National Oceanic 317
 and Atmospheric Administration Earth System Research Laboratory 318
 (NOAA-ESRL) ([http://www.esrl.noaa.gov/psd/data/climateindices/](http://www.esrl.noaa.gov/psd/data/climateindices/list/)
 319 [list/](http://www.esrl.noaa.gov/psd/data/climateindices/list/)). The period of analysis used to setup the long-term forecasting 320
 model extended from 1980 to 2018, while that for short-term weather 321
 forecasting ranged from 2007 to 2018. 322

323 **III. METHODS**

324 The general approach followed in this study and the experimental 324
 components are schematically shown in [Fig. 3](#). The following sections 325
 describe the methodological components in detail. 326

327 **A. Short-term ensemble flow forecasting**

328 To obtain the short-term forecasts for the lead time of 7 days for 328
 inflow into each of the three reservoirs in the dam network, two kinds 329
 of models were incorporated: (i) data-based artificial neural network 330
 (ANN) model for the Blue Mesa dam, which is the most upstream in 331
 the multi-dam network and (ii) linear regression model for the 332
 Morrow Point and Crystal dams, which lies downstream. The ANN 333
 model was specifically chosen for the Blue Mesa dam because it 334
 receives most of the unregulated flow and the nonlinearities in the 335
 hydrological response are most suited for a complex model like ANN. 336
 However, for the next two downstream dams, the inflows are highly 337
 dependent on the release from the upstream dam and hence do not 338
 require complex modeling exercise. As the skill in modeling the system 339
 inflow is mostly driven by the most upstream Blue Mesa dam; the 340
 focus was to improve the quality of Blue Mesa's forecast inflow using 341
 ANN. The specifications of the ANN model are described next 342

AQ3

AQ4

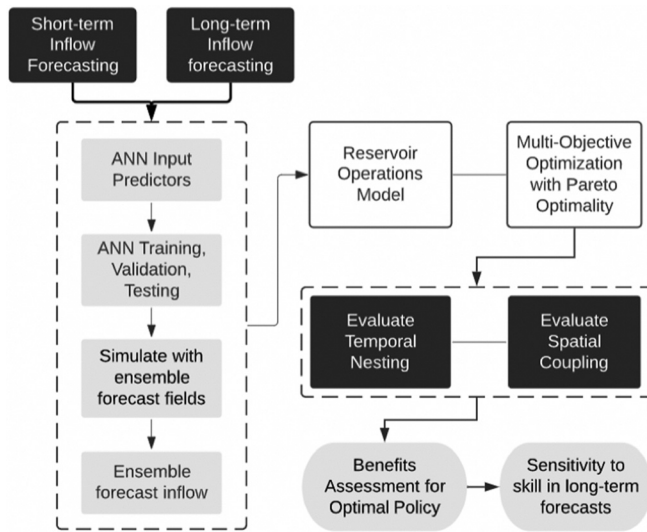


FIG. 3. Schematic of the approach showing key experimental components of the study. See Table IV for explanation of the evaluation framework strategies.

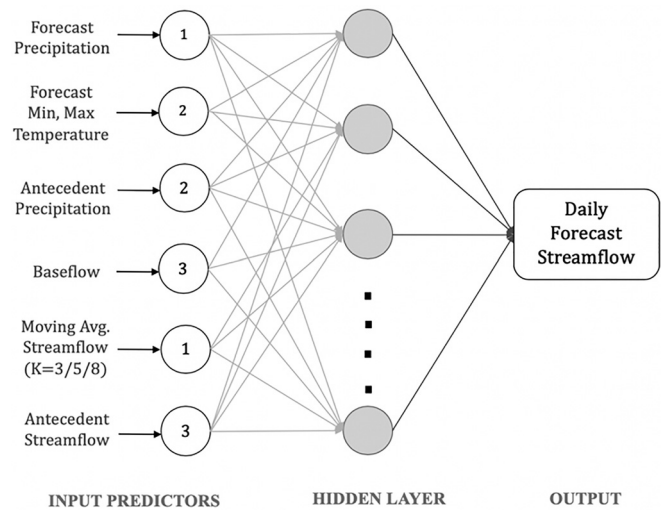


FIG. 4. ANN model configuration with the selected input predictors for daily streamflow forecasting over the Blue Mesa dam. Log sigmoid and linear transfer functions were used for hidden and output layers, respectively. The number of antecedent/forecast days for each node is also shown. K is the window length for moving average streamflow that varies with the forecast lead time.

343 followed by the linear regression model and ensemble forecast
344 processing.

345 **1. ANN model for daily flow forecasting**

346 The daily forecasting model is based on a feedforward neural
347 network involving input, hidden, and output layers. Considering
348 the reservoir and basin characteristics, the candidate input layer
349 nodes were identified as: (i) forecast fields of precipitation and
350 temperature, obtained from the GFS model at a resolution of 0.5°;
351 (ii) antecedent precipitation over the basin; (iii) antecedent
352 streamflow into the reservoir; and (iv) antecedent baseflow. A pro-
353 cedure was followed similar to that used by Ahmad and Hossain
354 (2019) for selecting the optimal set of input predictors to this ANN
355 model. The final predictor set included antecedent precipitation
356 (2 days), antecedent baseflow (3 days), antecedent inflow (1/2/
357 3 days based on the lead time), antecedent moving average inflow
358 (3/5/8-day window based on the lead time), forecast precipitation
359 (1 day), and forecast min/max temperature (1 day each). The con-
360 figuration of the short-term ANN model is shown in Fig. 4. The
361 ANN was trained using the Levenberg–Marquardt (LM) method,
362 and measures of early stopped training (STA) and regularization
363 were taken to avoid overfitting and lack of generalization (underfit-
364 ting). The period of Jan 2007 to Aug 2014 was used as the training
365 set, while the validation and testing sets were selected as Sep
366 2014–Oct 2015 and Nov 2015–Dec 2017, respectively.

367 **2. Linear regression model for downstream dams**

368 Using the modeled inflow into the most upstream dam, a linear
369 regression model was developed to route the release from upstream
370 dams to inflow into the downstream reservoirs. The linear regression
371 model was deemed to be fit for the purpose as the two downstream
372 dams, Morrow Point and Crystal, mostly receive regulated flow with

minimal contribution from the intermediate tributaries. The two sets
of linear regression models were developed: (a) between Blue Mesa
release and Morrow Point inflow and (b) between Morrow Point
release and Crystal inflow. The linear relationships and the respective
correlations are shown in Fig. 5.

373 **3. Ensemble forecast processing**

374 After the base reservoir inflow models (ANN-based for Blue
375 Mesa and linear regression-based for other two dams) were developed
376 to obtain deterministic inflow forecasts for the lead time of 1–7 days,
377 the uncertainty in forecasts was modeled next for the Blue Mesa dam
378 inflow. The trained ANN model was fed with 11 ensemble scenarios
379 of the forecast forcings from the GEFS model to result in the ensemble
380 inflow forecast. Given that the reservoir operation model was designed
381 to use a deterministic optimization technique, the average scenario of
382 the ensemble forecast members was used in the optimization model
383 (see Sec. III C). The average of the ensemble flow forecasts showed
384 higher skill compared to the deterministic forecasts obtained using
385 GFS forcings (see Table V). The higher skill in the average scenario of
386 GEFS-based ensemble forecast flow as compared to the deterministic
387 daily forecasts from GFS was also confirmed in a study by Ahmad and
388 Hossain (2019) for multiple dams in US.

389 **B. Long-term ensemble flow forecasting**

390 For nesting the short-term optimization model with long-term
391 operations, the long-term flow forecast model was developed to result
392 in monthly inflow forecasts for up to 7-months in the future. Similar
393 to the short-term forecasting, a feedforward ANN model with one hid-
394 den layer was designed to forecast the inflow into the most upstream
395 Blue Mesa dam. However, an entirely different set of input predictors
396 from the NMME climate model outputs suitable to capture seasonal
397

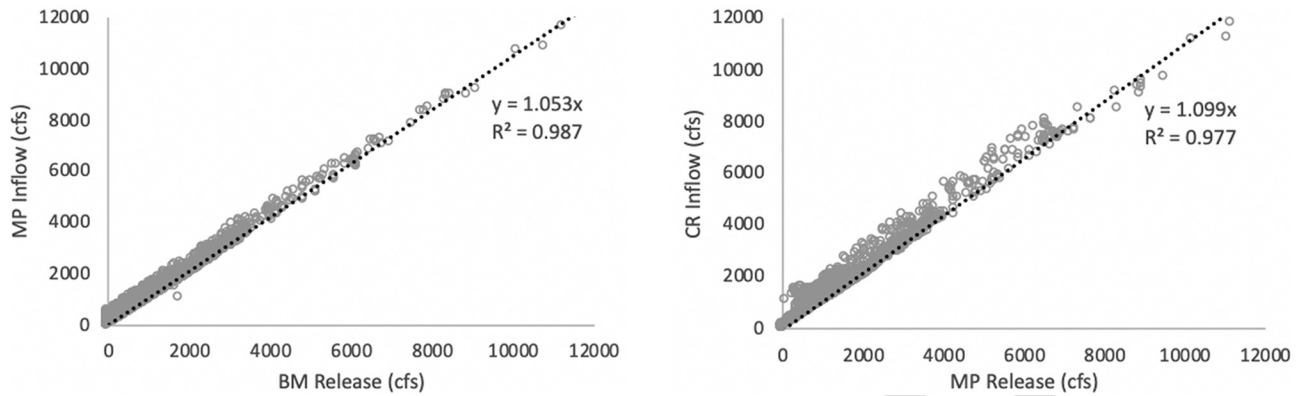


FIG. 5. Scatter plots showing linear regression between release and inflow of the upstream–downstream dam pairs of Blue Mesa (BM)–Morrow Point (MP) and Morrow Point (MP)–Crystal (CR) dams.

402 variations in seasonal runoff was developed. Based on a predictor selection
 403 analysis similar to that for the short-term ANN model, the input
 404 predictors were forecast precipitation (1 month; from the CFSv2 model),
 405 forecast sea surface temperature (1 month; from the GFDL CM2.1
 406 model), antecedent inflow (1/2/3 months based on the lead time), ante-
 407 cedent baseflow (3 months), antecedent moving average flow (3/5/8-
 408 month window based on the lead time), and Niño 3.4 index (1 month).
 409 The climate models in NMME contain 12 ensemble members (realizations)
 410 for each variable, which were used to train the ANN model. The
 411 average trace of the forecast flow was used for optimization. For the
 412 other two downstream dams, the linear regression model for daily fore-
 413 casting was used under the assumption that inflow contributions from
 414 tributaries at the monthly scale are insignificant. The available dataset
 415 was divided into *training*, *validation*, and *test* sets extending from 1981
 416 to 2007, 2008 to 2011, and 2012 to 2018, respectively.

417 **C. Reservoir operation optimization**

418 The forecast flow information obtained from short and long-
 419 term forecasting models was used as input to the optimization model
 420 for obtaining optimal release decisions. The focus of this study was on
 421 hydropower maximization, which was formulated as the major objec-
 422 tive. Other constraints were incorporated into the model representing
 423 flood control, environmental flow concerns, and dam safety. The
 424 short-term optimization model was setup with a daily temporal scale
 425 over the 7-day horizon, while the long-term model was developed to
 426 output optimal release decisions at the monthly scale with the opti-
 427 mization horizon of 7 months. The nesting of the two optimization mod-
 428 els was carried out by using the long-term optimal reservoir state to
 429 formulate a complementary objective function into the short-term
 430 model at every time step of the horizon. Different operation strategies
 431 were devised to evaluate the value in co-optimization. The long-term
 432 optimization model is described next, which is the basis for the nesting
 433 procedure, followed by short-term optimization and evaluation
 434 strategies.

435 **1. Long-term optimization model**

436 The optimization model for monthly release decisions is based
 437 on two objective functions, maximizing the total hydropower

generation from all power plants in the system and minimizing the 438
 deviation of elevation of the Blue Mesa dam at the end of year from a 439
 required target level. As the skill in long-term forecasts degrades with 440
 the increasing lead time, the model predictive scheme (MPC) was 441
 employed at the monthly scale, which updates the flow forecasts at 442
 every step of the optimization horizon (Turner *et al.*, 2017; Ahmad 443
 and Hossain, 2020). The spread of the ensemble flow forecasts was 444
 ignored in the deterministic optimization procedure so that it can pro- 445
 vide a clear indication of the contribution of forecasts to the optimal 446
 operation performance (Turner *et al.*, 2017). 447

The two objectives are formulated below: 448

- 449 1. Maximizing hydroelectric power production (MW) from the sys- 449
 tem’s three power plants, 450

$$\max f_1(MW) = \sum_n \sum_t \epsilon^n \cdot \Delta t_{turb}^n \cdot (HF_t^n - HT_t^n) \cdot R_{p,t}^n, \quad (1)$$

where t is the optimization horizon of 7 months, n is the index 451
 for the reservoir in consideration, $n = 1, 2, 3$, HF and HT are the 452
 reservoir forebay and tailrace water levels (ft), ϵ is the turbine 453
 efficiency, Δt_{turb} denotes the turbine operating hours, and R_p is 454
 the power release from turbines (cfs). 455

- 456 2. Minimizing the absolute value of deviation of reservoir elevation 456
 from the target level (T) in the month of December (H_{Dec}) for 457
 the Blue Mesa dam. This is to satisfy the requirement for the 458
 Blue Mesa dam to return to 7490 ft on December 31st to provide 459
 storage for next spring’s runoff and minimize upstream icing. 460
 Under the MPC scheme of optimization, the objective is only 461
 implemented for horizons containing the month of December. 462

$$\min f_2(ft) = . \quad (2)$$

The energy production function in Eq. (1) requires the knowl- 463
 edge of turbine efficiency and the number of operating hours for 464
 everyday operations. Because the turbine operating characteristics usu- 465
 ally vary over the year and within any day of operations, a regression 466
 model was developed for estimating energy generation. Linear regres- 467
 sion was performed between the observed hydropower (in MWh) 468
 and the product of hydraulic head ΔH and power release R_p based on 469
 the historical data. The obtained regression constant captures the 470

471 unknown turbine efficiency ϵ and operating hours Δt_{turb} . The con-
472 stants were obtained as 17.02 h, 18.64 h, and 12.22 h for Blue Mesa,
473 Morrow Point, and Crystal dams, respectively. Multiple constraints
474 were imposed on the long-term optimization model considering flood
475 control, dam safety, environmental flow requirements, and operational
476 restrictions for Aspinall reservoirs specified in the control manuals.
477 Various operational restrictions specified by the control manuals
478 (USBR, 2004, 2012a, 2012b) (see Sec. II A) were considered for setting
479 up the constraints as summarized in Table II.

480 2. Short-term daily optimization model

481 The daily-scale multi-objective optimization model using the
482 MPC scheme was setup to generate optimal release decisions for one
483 week ahead in the future. The primary and secondary objectives varied
484 with the strategy of optimization (see Table IV). The ensemble forecast
485 spread was ignored during the optimization for reasons mentioned
486 under the long-term optimization model. The constraints for optimi-
487 zation were tailored to account for the daily-scale reservoir operations
488 of the three dams. In addition to the constraints for the long-term
489 optimization model, the daily ramping rates for Crystal dam release
490 and daily maximum change in the Crystal reservoir forebay elevations
491 were constrained by the values specified in the control manuals and
492 are summarized in Table III.

493 3. Optimization algorithm

494 The multi-objective optimization problem was solved using
495 deterministic genetic algorithm-based optimization. Due to the con-
496 flicting nature of objective functions, a non-dominated or Pareto set of
497 solutions is needed where one objective function cannot be improved
498 further without violating the other. To implement the Pareto optimal-
499 ity, the Non-dominated Sorting Genetic Algorithm (NSGA-II;
500 Deb et al., 2002) was used. Open-source library *platypus*

TABLE II. Dam-specific and general constraints imposed on the monthly optimization model.

Dam-specific constraints	Value
Blue Mesa Dam	
Minimum elevation	7393.0 ft
Maximum elevation (Jan–Mar)	7490.0 ft
Maximum elevation (Apr–Dec)	7519.4 ft
Elevation on Dec 31	7490.0 ft
Morrow point dam	
Minimum elevation (Jun–Sep)	7151.0 ft
Minimum elevation (Oct–May)	7143.0 ft
Maximum elevation	7160.0 ft
Crystal dam	
Minimum elevation	6725.0 ft
Maximum elevation	6772.0 ft
General constraints	
Minimum monthly release	2500 cfs
Maximum monthly release	64 500 cfs
Maximum monthly release (May 10–Jun 1)	220 000 cfs

TABLE III. Additional constraints imposed on the daily scale short-term optimization model.

Dam-specific constraints	Value
Crystal dam	
Maximum elevation change (Apr–Jun)	4 ft per day
Maximum elevation change (Jul–Mar)	10 ft per day
Daily ramping rate—increase	500 acre-ft per day
Daily ramping rate—decrease	400 acre-ft per day
Morrow point dam	
Daily ramping rate—increase/decrease	2000 acre-ft per day
Blue Mesa dam	
Daily ramping rate—increase/decrease	2000 acre-ft per day
General constraints	
Minimum daily release	300 cfs
Maximum daily release	2150 cfs
Maximum daily release (May 10–Jun 1)	12500 cfs

(<https://platypus.readthedocs.io>) was incorporated to formulate the
501 multi-dam optimization problem. The algorithm produces a set of
502 Pareto optimal solutions (with the user-defined size of Pareto optimal
503 set), from which the dam operator can choose the preferred solution
504 based on which objective function receives priority according to the
505 situation at hand. For the sake of this study, a balanced optimal solu-
506 tion was selected on the Pareto front that gives equal weightage to
507 both the objectives. Pareto optimization allows for different units of
508 objective functions without the need to transform to consistent units,
509 which is often difficult to achieve (Madsen et al., 2009). 510

511 D. Co-optimization at long-term and short-term scales

512 The proposed strategy optimizes the operations of the cascade of
513 dams in tandem while considering the long-term benefits for short-
514 term optimality. We coin this co-optimization as *temporal nesting*
515 *with spatial coupling* (TeNeSC). TeNeSC-based optimization is carried
516 out in two steps; first, the long-term model, as described in Sec. III C 1,
517 is used to obtain monthly optimal release decisions over an optimiza-
518 tion horizon of seven months into the future. The monthly optimal
519 operations yield the optimal reservoir states at the end of each month.
520 The end-of-month reservoir storages over the 7-month horizon are
521 linearly interpolated to result in the daily levels that form the boundary
522 conditions or constraints for the short-term daily scale optimization
523 model. The small storage of dams in consideration (capacity to the
524 annual inflow ratio close to 1) results in variability in the reservoir state
525 at daily scales and justifies the daily time step for short-term optimiza-
526 tion (Anghileri et al., 2016). Furthermore, the “coupled” component
527 in the TeNeSC scheme signifies the joint operation of the dam net-
528 work, where the co-optimization is carried out by simultaneously con-
529 sidering releases from all the dams. The water released from the
530 upstream dam reaches the downstream reservoir with a certain delay
531 equal to the flow travel time along the reach. The delay time usually
532 ranges from several hours and extends to days only when the flow
533 travel time is long enough in large multi-reservoir systems (Souza and
534 Diniz, 2012; Ge et al., 2014). Given that the present study considers
535 daily scale operations over medium scale inter-reservoir reaches, the

536 delay time was neglected in the routing of streamflow. A schematic
 537 illustrating the temporal nesting of the optimization models is shown
 538 in Fig. 6.

539 The boundary conditions were used to formulate the secondary
 540 objective for the short-term optimization model where the primary
 541 goal is hydropower maximization across all the dams in the network.
 542 The objective was set to minimize the deviation of elevation from the
 543 boundary conditions (or target elevation) reflecting the long-term
 544 optimal conditions over the short-term optimization horizon. Because
 545 the main purpose of the Crystal dam is to act as a regulator of the
 546 upstream releases, there is a lesser flexibility left for the optimal reser-
 547 voir level for hydropower maximization. This was taken into consider-
 548 ation by obtaining the deviation of reservoir levels only on the first day
 549 of the optimization horizon. The higher weight is indirectly assigned
 550 to the secondary objective as the MPC scheme only considers the first
 551 day's optimal release and discards the rest. However, for Blue Mesa
 552 and Morrow Point dams, the deviation was obtained at the last (sev-
 553 enth) day of the horizon as they are operated for peaking power and
 554 permit higher flexibility in operations. Mathematically, the secondary
 555 objective is formulated as

$$\min f_2(f_t) = |H_7^1 - T_7^1| + |H_7^2 - T_7^2| + |H_1^3 - T_1^3|, \quad (3)$$

556 where H_i^n is the n th reservoir's storage (numbered from the upstream
 557 to downstream dam) at time step t . The optimization problem was
 558 bound by the fundamental long and short-term constraints on reser-
 559 voir storages and releases described in Secs. III C 1 and III C 2. Apart
 560 from those, the continuity constraints for the three reservoirs over
 561 each time step t of the optimization horizon can be mathematically
 562 stated in vector form as

$$S_i(t + 1) = S_i(t) + I_i(t) + M.R_i(t), \quad (4)$$

563 where $S_i(t)$ is the vector of storages in reservoirs $i = 1, \dots, n$; $I_i(t)$
 564 and $R_i(t)$ are vectors of inflows into and release from each reservoir;
 565 and M is an $n \times n$ square matrix representing the indices of reservoir
 566 connections,

$$M = \begin{bmatrix} -1 & 0 & 0 \\ 1 & -1 & 0 \\ 0 & 1 & -1 \end{bmatrix}$$

For the continuity constraints, storage-elevation relations were
 obtained as second-order polynomial equations for each reservoir
 using 15 years of historical data (2004–2018) using which the storage
 at each time step was converted to the respective reservoir level. The
 coupled optimization model solves a giant matrix for all the reservoirs
 to derive the optimal reservoir release decisions and their respective
 states at each time step.

E. Evaluation framework for co-optimization 574

To answer the first research question of this study and establish
 the efficacy of co-optimization, several strategies of optimization were
 implemented under an evaluation framework. The objective is to sepa-
 rately underscore the value in two different facets of co-optimization
 for maximizing hydropower: (a) nesting of short- and long-term
 objectives in time and (b) coupling of reservoirs in space. Tables IV(a)
 and IV(b) summarize the specifications of each strategy for evaluating
 temporal nesting and spatial coupling.

An additional aspect that needs consideration for demonstrating
 the robustness of this concept is the value of the real-time forecasting
 model in improving the operational benefits of the dam network. Our
 study accomplishes this by considering two different scenarios of
 obtaining the inflow forecasts:

- (a) *perfect forecast scenario* that stands as a hypothetical bench-
 mark of maximum attainable benefits using the different
 strategies described above. Here, the observed inflow is used
 as a proxy to the forecasts over the desired optimization hori-
 zon to simulate the perfect forecast scenario.
- (b) *operational forecast scenario* where the reservoir inflow fore-
 casts are obtained using the short- and long-term forecasting
 models developed in Secs. III A and III B. This scenario is the
 representative of the practically possible benefits using an

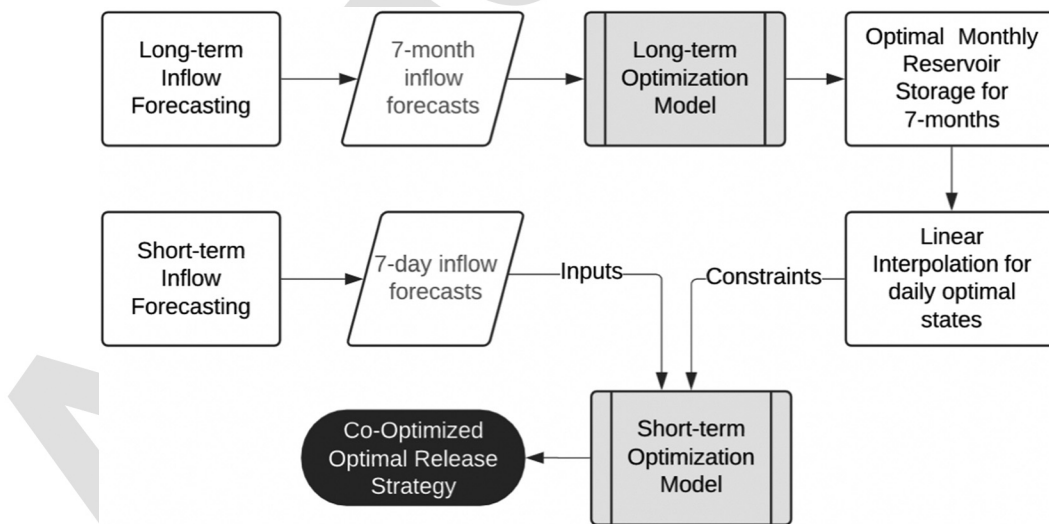


FIG. 6. Schematic explaining the procedure of co-optimization with the long- and short-term objectives.

TABLE IV. (a) Specifics of strategies under the framework to evaluate the value in temporal nesting, formulated as the multi-objective problem. (b) Specifics of strategies under the framework to evaluate the value in spatial coupling.

Strategy	Formulation	Description	Objective
(a) All Spatially Coupled TeNeSC	Short + long	<ul style="list-style-type: none"> • Uses nested co-optimization at long and short-term scales • Continuity constraints formulated as one giant matrix [Eq. (4)] 	<p><i>Primary:</i> maximize hydropower</p> <p><i>Secondary:</i> minimize the deviation of reservoir elevation from target levels based on long-term optimality [Eq. (3)]</p>
T1	Short-only	<ul style="list-style-type: none"> • No use of nested co-optimization • Continuity constraints the same as TeNeSC 	<p><i>Primary:</i> maximize hydropower</p> <p><i>Secondary:</i> minimize the absolute deviation between reservoir release and turbine capacity: $\min f_2(cfs) = \sum_{i=1}^n \sum_{t=1}^T R_t^i - T_{cap}^i$ (n: number of reservoirs; T: short-term horizon of 7 days).</p>
T2	Long-only	<ul style="list-style-type: none"> • No use of nested co-optimization • Considers long-term optimality only during daily optimization • Continuity constraints the same as TeNeSC 	<p><i>Primary:</i> minimize the absolute deviation of reservoir elevation H from target levels based on long-term optimality T for the first day of horizon $\min f_1(ft) = \sum_{i=1}^n H_1^i - T_1^i$ (n: number of reservoirs)</p> <p><i>Secondary:</i> the same as the secondary objective in T1</p>
(b) Both Temporally Nested TeNeSC C1	Coupling No coupling	<ul style="list-style-type: none"> • The same as in Table IV(a) • No coordination among reservoir release decisions. • Separate optimization models developed for each reservoir; the regression model converts upstream release into downstream inflow 	<p>Same as in Table IV(a)</p> <p><i>Primary:</i> maximize hydropower</p> <p><i>Secondary:</i> the same as TeNeSC, deviation calculated individually for each reservoir in the respective optimization model</p>

operational flow forecasting. The technique is operational for real-time reservoir inflow forecasts for Ganges and Brahmaputra river basins (Ahmad and Hossain 2019; http://depts.washington.edu/saswe/datavis_Timeseries.html).

601 F. Benchmark scheme

To obtain the actual value in using forecast information for realizing optimal operations, a benchmark operating scheme is necessary that by itself neither uses any forecast information nor is based upon any co-optimization at different timescales. Rather, the benchmark scheme should be reflective of control rules designed with respect to certain operating objectives that the dam operator follows in practice. Thus, to setup a fair benchmark, a customized control-rule based operation scheme was designed to specifically address the hydropower maximization objective (Turner et al., 2017), which is also the basis of strategies described under the evaluation framework. The control rules were designed in the form of lookup table where the optimal release is specified as a function of two state variables: reservoir storage and season of year, as proposed by Turner et al. (2017). The stochastic

dynamic programming (SDP)-based optimization procedure coded in the R package *reservoir* (Turner and Galelli, 2016) was incorporated to optimize for these rules. The observed inflows for 15-year period (2004–2018) were used for each dam as input to the SDP model, including the reservoir and objective function specifications. Three separate sets of control rules were obtained for each reservoir at the monthly time step, with no coupling between the operations of adjacent reservoirs. To assess the benefits against this benchmark, a metric called *percent improvement over benchmark* (IB) was formulated as

$$IB (\%) = \frac{HP_{optim} - HP_{bm}}{HP_{bm}} \times 100, \tag{5}$$

where HP_{optim} and HP_{bm} are the total hydropower production (HP) from the three dams of the Aspinall Unit using optimized and benchmark reservoir operating schemes.

627 G. Effect of skill in long-term forecasts

The skill in long-term monthly flow forecasts usually degrades rapidly as compared to that in the short-term daily-scale forecasts. As the temporal nesting uses long-term forecasts as the boundary

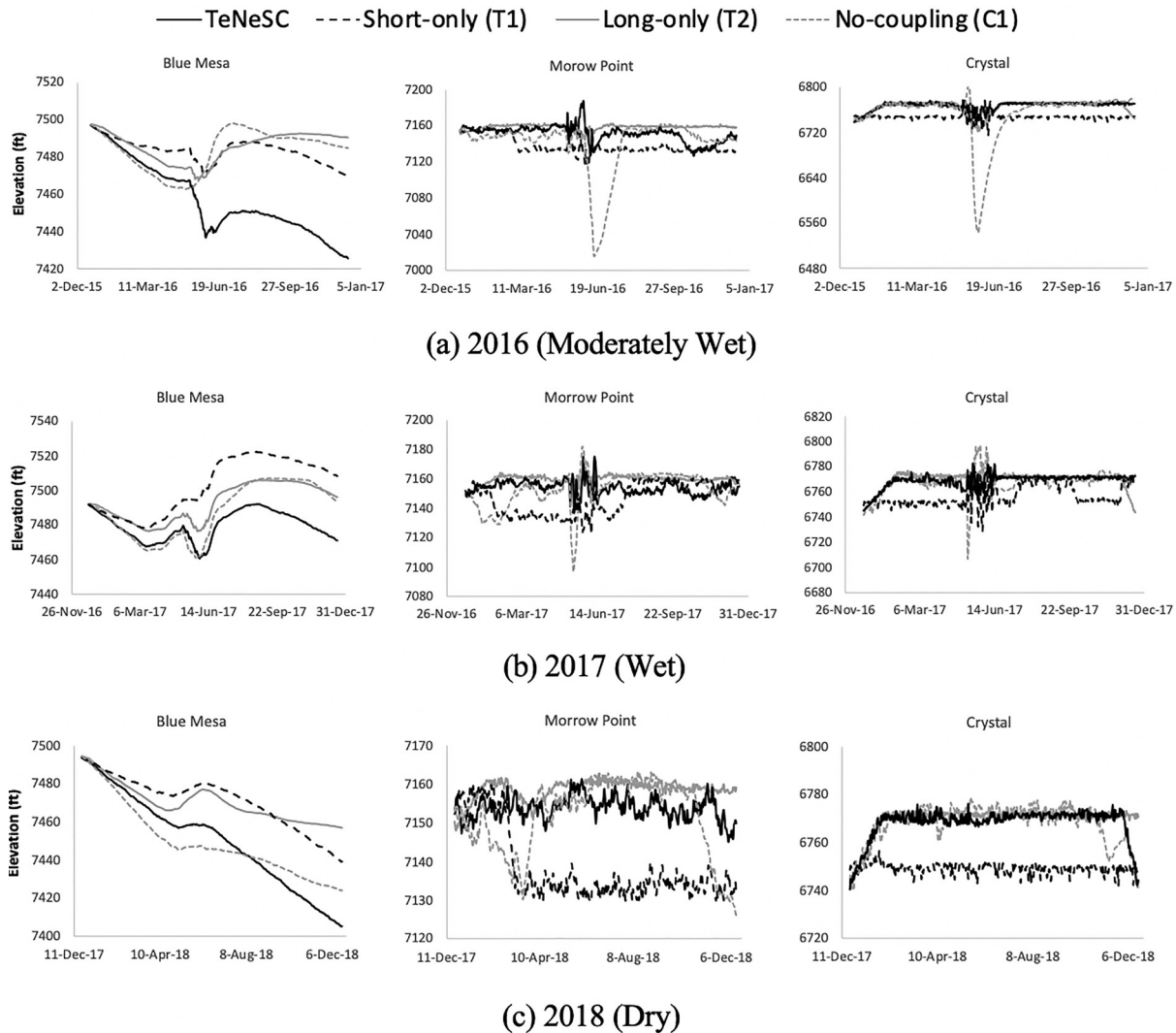


FIG. 7. Optimal reservoir elevations from the different strategies using the perfect forecast scenario for the three dams over the three years with different flow characteristics.

631 condition for the daily-scale optimization model, the performance is
 632 primarily driven by the skill in the long-term forecasts. For instance,
 633 any major error in predicting the onset of flood or drought season can
 634 cause the short-term release decisions to be optimized toward an
 635 objective function that does not reflect long-term optimality. This can
 636 potentially result in sub-optimal operations in both the short and long
 637 terms. Hence, it is imperative to assess how the skill in monthly ANN-
 638 based forecasts affects the resulting optimal reservoir operation policy.

639 The observed monthly inflow data were synthetically corrupted
 640 to simulate underestimation and overestimation in the flow forecasts.
 641 Six perturbed monthly inflow timeseries were generated by adding
 642 multiplicative bias with six different constants, three of which simu-
 643 lated underestimation (multiplicative constant < 1), while the rest simu-
 644 lated overestimation in the predicted inflow (multiplicative
 645 constant > 1). The multiplicative factors simulate the worst-case sce-
 646 narios of consistent over- or under-prediction of the flows across the

period of analysis. Also, as the forecast error is more likely to increase
 for higher river flows (Montanari and Grossi, 2008), the proposed factors
 were able to replicate increasing bias in forecasts for higher inflow.
 Perturbed monthly inflow timeseries were used to carry out the co-
 optimization (TeNeSC) using the perfect short-term inflow forecasts.
 The resulting reservoir elevations and hydropower benefits were com-
 pared across the different perturbed scenarios to assess the effect of
 degrading skill in long-term predictions.

IV. CASE STUDY RESULTS

A. Reservoir operation optimization

The proposed concept of co-optimization and strategies for eval-
 uation were implemented over the selected multi-dam network of the
 Aspinall Unit of Blue Mesa, Morrow Point, and Crystal dams. Three
 years (2016–2018) with different inflow characteristics were selected
 for the analysis. While 2016 was a moderately wet year with the annual

662 inflow of 441 535 cfs into the system, 2017 and 2018 experienced
 663 anomalously wet and dry conditions with the annual inflow of
 664 629 083 cfs and 211 853 cfs, respectively. The different flow conditions
 665 were chosen to further underscore the robustness of this technique
 666 under different seasons of dam operations. The detailed results are
 667 described in the following sections. The assessment of the forecast skill
 668 in short and long-term ANN flow forecasting models is described in
 669 detail in Appendix for the interested readers.

670 **1. Evaluation framework**

671 The long-term optimal policy derived from the monthly scale
 672 optimization model was used for the strategies that nest long-term
 673 benefits with short-term optimization (i.e., TeNeSC and C1). For the
 674 other strategies used for evaluation, either only the short-term fore-
 675 casts (T1) or long-term forecasts (T2) were used for the optimization.
 676 Figure 7 shows the optimal reservoir elevations using these strategies
 677 using perfect forecasts for the three years, while Fig. 8 shows the

678 corresponding optimal elevations obtained using the operational fore-
 679 casts (ANN-based for Blue Mesa and regression-based for the others).
 680 The long-term optimal policy of operations is also shown alongside in
 681 each plot.

682 When the optimization model uses temporal nesting and consid-
 683 ers the three reservoirs as a network (TeNeSC), the reservoir levels
 684 from the short-term optimization model are adjusted according to
 685 closely follow the long-term optimality. The long-term optimal policy
 686 tends to maximize the reservoir storage for the downstream two dams,
 687 where the upstream Blue Mesa dam acts as buffer for maximizing the
 688 energy generation. The resulting flexibility in the operation of
 689 upstream dams enables them to provide peaking power, while the
 690 Crystal dam traces the long-term optimal levels with minimal changes
 691 in reservoir levels. Considering the strategies used to evaluate TeNeSC,
 692 the short-term optimization (T1) results in lower storage levels for the
 693 downstream dams, resulting in lower hydropower benefits in the long-
 694 run due to its myopic nature. In contrast, the long-term only strategy
 695 (T2) tends to closely trace the monthly target levels but loses additional

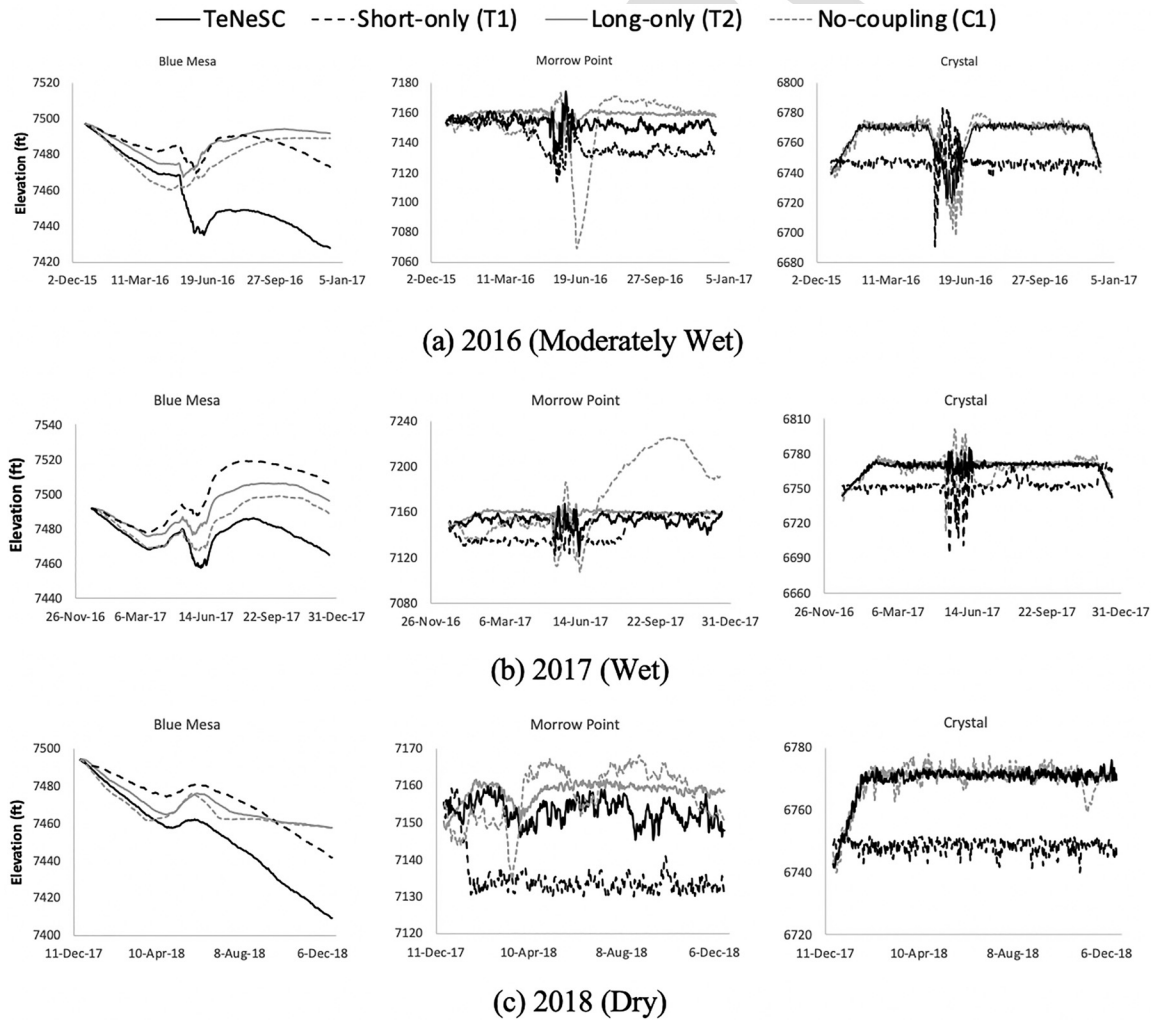


FIG. 8. Optimal reservoir elevations from different strategies using operational forecasts (ANN/linear regression-based) for the three dams.

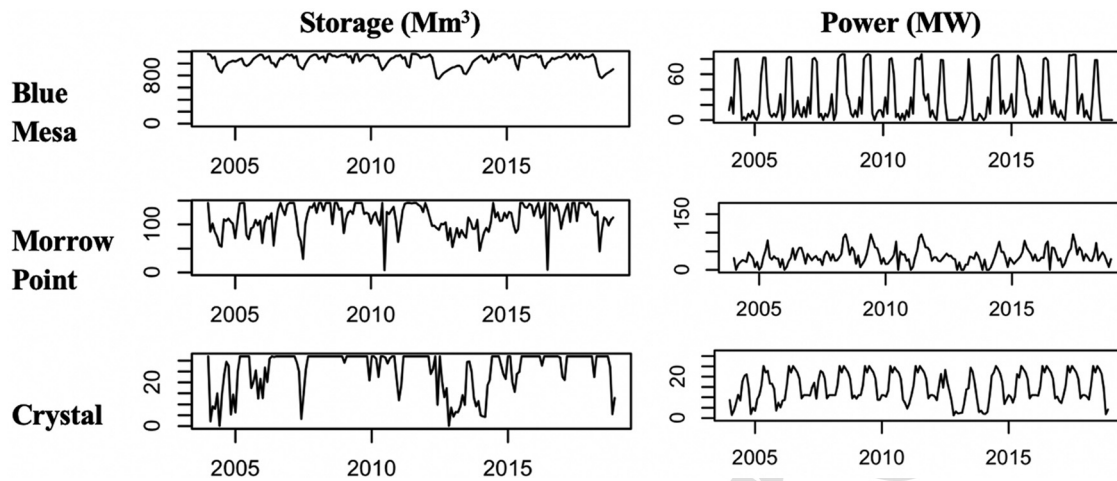


FIG. 9. Benchmark control rules designed specifically for hydropower maximization using the R package *reservoir* for the dams in the Aspinall Unit during the period 2004–2018 at the monthly scale (after Turner and Galelli, 2016).

696 hydropower benefits in short-term possible by tweaking the daily
697 release decisions accordingly (Table V).

698 Further, the value in spatial coupling was assessed separately by
699 comparing TeNeSC with the no-coupling scenario (no co-ordination
700 among reservoir release decisions; C1). The results from C1 suggest
701 that one of the two downstream dams undergoes major fluctuations in
702 reservoir levels, even violating the storage constraints for a few days
703 irrespective of co-optimization at the long- and short-term scales. The
704 fluctuations primarily occur during the peak flow season of wet years.
705 In contrast, spatial coupling of dams further facilitates in keeping the
706 reservoir levels within safe bounds and prevents violation of the stor-
707 age constraints. TeNeSC helped avoid any sudden surge or steep dip
708 in the reservoir levels during the wet and dry years. Finally, the high
709 accuracy of operational forecasts leads to optimal policies similar to
710 those obtained by the use of perfect forecasts (see Fig. 8).

711 **2. Benchmark scheme**

712 The reservoir storage and resulting hydropower generation
713 (MW) using the benchmark scheme are shown in Fig. 9 for the three
714 dams. The scheme is derived individually for each dam in the network
715 based on the observations over 2004–2018, without using any forecast
716 information.

717 **3. Hydropower benefit assessment**

718 The hydropower benefits harnessed from each strategy over the
719 three years and using the two forecast scenarios are shown in Table V.
720 The benefits from the perfect forecast scenario set bounds to maxi-
721 mum attainable benefits, which cannot be exceeded by the optimal
722 policy under the operational forecast scenario. Hydropower generation
723 (MWh) using observed real-world operations (obtained from USBR)
724 is also shown in Table V for comparison.

725 The high skill in ANN forecasts resulted in benefits similar and
726 lesser to those from the perfect forecast scenario for all the strategies.
727 Considering the different years of analysis, the proposed approach of
728 TeNeSC, which answers the key research question of our study, is

more advantageous during the dry and moderate years (2016 and 729
2018) as compared to the wet year (2017). 730

731 Within the strategies evaluating values in temporal nesting, both
732 the short-term-only (T1) and long-term-only (T2) optimization result
733 in lower benefits in hydropower when compared against the proposed
734 benchmark. TeNeSC, on the other hand, generates benefits of 734
14%–41% over the different seasons for the perfect forecast scenario. 735
Further, using the short-only optimization (T1) was most beneficial 736
for drier years, while the long-term only optimization (T2) produced 737
more benefits for the wetter year. This stresses the value in incorporat- 738
ing both the strategic and tactical planning for robustly efficient opera- 739
tions across different years. Next, the value in spatial coupling is 740
underscored by comparing TeNeSC against strategy C1 with no cou- 741
pling. The latter again falls short of the hydropower benefits compared 742
to the former. This is because when the optimization considers only 743
the individual reservoirs without any coordination in release decisions, 744
the optimal policy for one dam leads to other dams performing sub- 745
optimally, leading to an overall reduced performance of the system. 746
The hydropower generation from real-world observed operations, 747
although not used for assessment as mentioned in Sec. III F, was com- 748
parable to those from the benchmark scheme. 749

750 **B. Effect of skill in long-term forecasts**

751 The perturbed inflow forecasts for the Blue Mesa dam were
752 obtained for the moderately wet year of 2016 to study the effect of skill
753 in monthly forecasts on the optimal operations. Figure 10(a) shows
754 the perturbed inflow time series using six different constants of multi-
755 plicative bias. The long-term optimization model was first used to
756 obtain monthly optimal policies for the three dams. Figure 10(b)
757 shows the optimal long-term policy for the Blue Mesa dam for the cor-
758 responding perturbed inflow time series.

759 The long-term optimal elevations were then used to constrain the
760 short-term optimization under the TeNeSC scheme. The hydropower
761 benefits using the optimal operating policy from different underesti-
762 mation and overestimation scenarios are summarized in Table VI.
763 Comparing the outputs from different scenarios of perturbation, a

AQ5

TABLE V. Assessment of hydropower production (HP) benefits over the Aspinall unit using different strategies compared against benchmark and observed benefits over three years; IB is the improvement in production over the benchmark scheme. Comparing TeNeSC with T1 and T2 gives values in temporal nesting, while comparing with C1 gives values in spatial coupling.

Year	Strategy	Formulation	HP (GWh-perfect forecast)	IB (%)	HP (GWh-operational forecast)	IB (%)
2017 (wet)	TeNeSC	Short + long + coupled	1028	14.8	1021	14.1
	T1	Short-only	893	-0.3	877	-2.0
	T2	Long-only	934	4.3	929	3.8
	C1	Uncoupled	921	2.8	915	2.2
		<i>Benchmark</i>	895		...	
		<i>Observed</i>	812		...	
2016(moderate wet)	TeNeSC	Short + long + coupled	974	26.9	948	23.5
	T1	Short-only	837	9.0	821	7.0
	T2	Long-only	759	-1.1	750	-2.3
	C1	Uncoupled	807	5.2	780	1.7
		<i>Benchmark</i>	767		...	
		<i>Observed</i>	761		...	
2018 (dry)	TeNeSC	Short + long + coupled	847	41.5	829	38.5
	T1	Short-only	684	14.3	669	11.8
	T2	Long-only	603	0.6	599	0.1
	C1	Uncoupled	702	17.2	652	8.9
		<i>Benchmark</i>	599		...	
		<i>Observed</i>	609		...	

764 higher bias of the inflow forecasts toward over- or underestimation
 765 generally results in lower energy benefits relative to the perfect
 766 forecast benefits. The effect of degrading skill is more prominent
 767 for the overestimation scenarios where the optimization strategy
 768 results in the over-conservative release policy, leading to lower
 769 energy production. The underestimation scenarios, on the other
 770 hand, yield relatively high releases and generate more energy when
 771 assessed over the entire year. However, the overall difference
 772 among the resulting optimal policies and respective hydropower
 773 benefits was insignificant. This is partly because the long-term

forecasts are not directly utilized for arriving at the final optimized
 releases; rather, the first step of long-term optimization leads to
 the monthly optimal release policy, which then feeds the daily
 optimization. Thus, the effect of poor skill in monthly forecasts is,
 to some extent, compensated for by the more accurate short-term
 forecasts while deriving the final daily optimal releases. This is
 advantageous in the case when long-term forecasts are not very
 skillful as demonstrated here with heavy over/underestimation,
 further underscoring the value of co-optimization at long- and
 short-time scales.

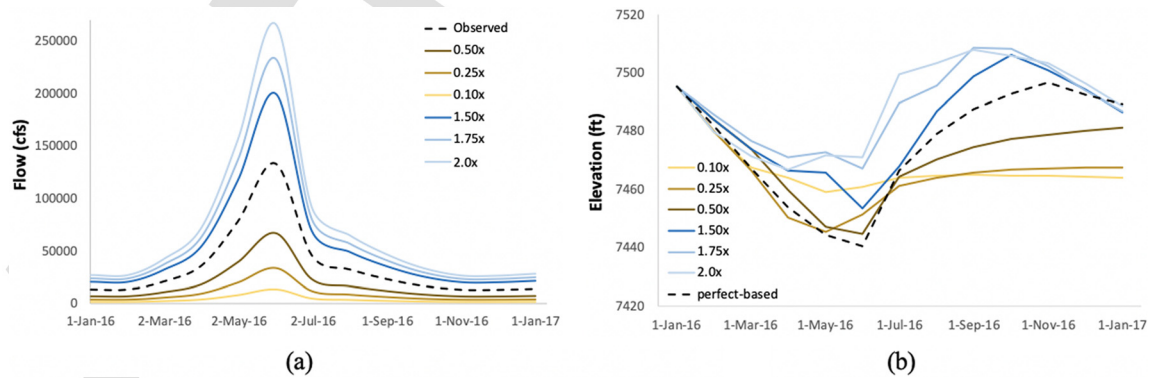


FIG. 10. (a) Perturbed inflow timeseries for the Blue Mesa dam over 2016 to be used for the TeNeSC scheme; (b) optimal monthly elevations for the Blue Mesa dam using the long-term optimization model based on the different perturbed forecast inflow time series; the black dashed line is based on perfect forecasts (i.e., observed inflow).

TABLE VI. Hydropower benefits obtained with TeNeSC using different perturbed inflow scenarios, "Nx" represents the perturbed inflow scenario obtained by multiplying the observed inflow timeseries by constant "N."

Underestimation scenario	Hydropower (GWh)	Overestimation scenario	Hydropower (GWh)
0.10×	968.1	1.50×	949.4
0.25×	973.4	1.75×	949.9
0.50×	960.8	2.0×	937.9
<i>Perfect forecast</i>	973.8		

784 V. DISCUSSION AND CONCLUSIONS

785 The smart use of skillful forecasts at weather and climate
786 scales can potentially make the operation of existing dams more
787 efficient. As forecast systems require fewer resources and man-
788 power than building new energy infrastructure (Turner *et al.*,
789 2017), a major implication of using the forecasts is the improved
790 efficiency of operations instead of building new hydropower dams
791 to satisfy the same energy demands. To realize this potential
792 toward energy generation, we have demonstrated a scheme that
793 integrates the long-term benefits with the short-term optimization
794 model to achieve optimality at both the time scales for a multiple
795 dam network. The findings presented here are globally applicable,
796 where energy demands and the need for greener and cleaner
797 energy production are simultaneously escalating.

798 As a first step, to model the reservoir short-term (daily) and
799 long-term (monthly) inflow forecasts, we used a numerically efficient
800 and skillful data-based technique of ANN for the most upstream dam
801 that receives unregulated natural flow. The publicly available NWP
802 forecast forcings at the weather scale and the climate model outputs at
803 the climate scale currently represent an underutilized resource for the
804 energy and water resource community. The data-intensive and skillful
805 ANN modeling technique was only employed for the most upstream
806 dam of the three-dam network that brings natural inflow into the sys-
807 tem. However, for the downstream reservoirs whose inflow is serially
808 correlated with releases from the respective upstream dams, a linear
809 regression model was found to be suitable for modeling the cascading
810 inflow. This concept can be useful even for more complex multi-dam
811 networks such as a parallel or combination of series-parallel networks,
812 where only the most upstream reservoirs (one or more) need a skillful
813 forecasting technique.

814 Our study shows that using the long-term optimal policy as a
815 guide to the short-term optimization model aids the reservoir in
816 avoiding any sudden surge or dip in the levels that might occur in
817 extreme seasons. In particular, this is valuable for the wet season
818 when an inflow peak with high uncertainty can leave the dam
819 operator with a small temporal window to pre-release and adjust
820 the reservoir levels when using short-term forecasts. With a skillful
821 monthly forecast of the inflow volume from climate models, the
822 temporal window of operations extends manifold giving the opera-
823 tor enough room to adjust the levels with minimal spells of heavy
824 spillway release. Similarly, during the extremely dry seasons, long-
825 term forecasts of drier years can keep the storage levels within safe
826 bounds for a relatively unvarying energy supply (satisfying the
827 baseload demands). The Pareto optimality in multi-objective

optimization provides flexibility to the dam operator to choose an
appropriate solution based on the prevailing circumstances and
trade-offs between the two conflicting objectives.

The other component of co-optimized operations is the spatial
coupling of reservoirs where the connected dams are operated and
optimized for in tandem. The results suggest that benefits to the dam
operator offered by coordination in release decisions depend on the
characteristics of the reservoirs in the network. A diverse network com-
prising reservoirs and power plants with varying characteristics can
potentially use the spatial coupling for the release policy tailored to
each dam. Thus, if a dam is assigned to meet base load demands, its
optimal release policy should allow for minimum changes in reservoir
levels while, for the dams whose purpose is to provide peaking power
during certain operational hours/days, the release policy can be
adjusted accordingly to maintain the requirements for other baseload-
providing reservoirs. This, when integrated with temporal nesting, has
far-reaching implications for the numerous small and large multi-dam
networks that were constructed in the previous centuries with long
service lives but are suffering from fading efficiencies. Our proof-of-
concept implies that smart use of seasonal and short-term forecasts can
compensate for the losses in performance and generate more energy.

The quantification of benefits under the evaluation framework was
performed by comparing them against a benchmark scheme that
completely neglects the forecasts. The study showed 14%–41% of
improvements in energy benefits from the co-optimized scheme against
the benchmark over years with different flow characteristics. In general,
the dry and medium years showed higher energy improvements than
the considered wet year. A similar conclusion was also reported by Xu
et al. (2014) who obtained long-term energy generation as a function of
short-term operations. As Xu *et al.* (2014) suggest, the objective of maxi-
mizing the hydropower or stored energy favors the long-term energy
production under drier conditions by maintaining higher storage levels.
This leads to relatively high overall improvements on nesting the short
and long-term optimality. However, wetter conditions demand higher
release, leading to a loss to the storage maximization objective in the
long term and hence comparatively lesser improvements to hydropower.

This study specifically focused on the application of forecast-
based reservoir operations at different temporal scales for improving
upon the hydropower generation. The technique involves components
of flow forecasting and optimization, which require *in situ* data on res-
ervoir operations and inflow for setting up the models. For operation-
alizing the concept over other dam networks across the globe, the
forecasting models can rely on inputs from the global NWP model
and satellite remote sensing. However, the optimization model needs
to be setup in conditions of scarce *in situ* data on dam operations. We
hope to consider this in a future study. Moreover, with improved effi-
ciency of reservoir operations, any excess energy generation can be
wasted if there is not enough demand for dispatching the power to the
grid, or in case, there is no provision for excess energy storage. Thus,
another logical future extension of this work is to integrate energy
demand forecasting and excess energy storage with the co-optimized-
based reservoir operations. The utility of nesting the weather forecasts
within the climate forecast-based operations not only is limited to
hydropower but can also benefit other renewables such as solar and
wind energy generation. Future endeavors on fostering the clean
energy generation should aim toward an integrated hydro-wind-solar
based energy framework.

AQ6

886 ACKNOWLEDGMENTS

887 This work was supported by the NASA Applied Science
 888 Program grant in Water Resources Nos. NNX15AC63G and
 889 NNX16AQ54G (Program Manager Dr. Bradley Doorn).

890 APPENDIX: SKILL ASSESSMENT IN FLOW
891 FORECASTING MODELS

893 1. Short-term inflow forecasts

894 Using the selected ANN architecture, the training, validation, and
 895 testing of the ANN base model were performed using the GFS forecast
 896 forcings for the Blue Mesa dam. The trained ANN model was then
 897 forced with 11-member ensemble forecast forcings from the GEFS
 898 model to result in the ensemble streamflow forecasts for lead times of
 899 1–7 days. The GEFS-based ensemble flow forecasts obtained using the
 900 trained ANN model are shown in Fig. 11 for the period of analysis
 901 2016–2018. The selected period of analysis included anomalously dry,
 902 intermediate, and anomalously wet years. The performance of the
 903 average scenario of GEFS-based ensemble forecasts is compared
 904 against that obtained using GFS-based forecast. The evaluation metrics

TABLE VII. Evaluation metrics comparing the GEFS-average and GFS based flow forecasts for lead times of 1, 4, and 7 days against the observed inflow for the Blue Mesa dam.

Metric	GEFS average scenario			GFS		
	L1	L4	L7	L1	L4	L7
NSE	0.971	0.923	0.912	0.972	0.921	0.888
Correlation	0.986	0.963	0.956	0.986	0.960	0.943
RMSE (cfs)	215.1	350.9	375.6	188.7	313.5	368.1
NRMSE	0.120	0.196	0.209	0.120	0.199	0.233

of Nash-Sutcliffe Efficiency (NSE), Correlation, Root Mean Squared Error (RMSE), and RMSE normalized with the mean of observed inflow (NRMSE) were used. The metrics are shown in Table VII.

The high accuracy exhibited by ANN flow forecasts results in a narrow spread of the GEFS-based ensemble forecasts. The average scenario of the ensemble has slightly higher skill as compared to that obtained from the GFS-based forecasts and hence was used as input to the short-term optimization model.

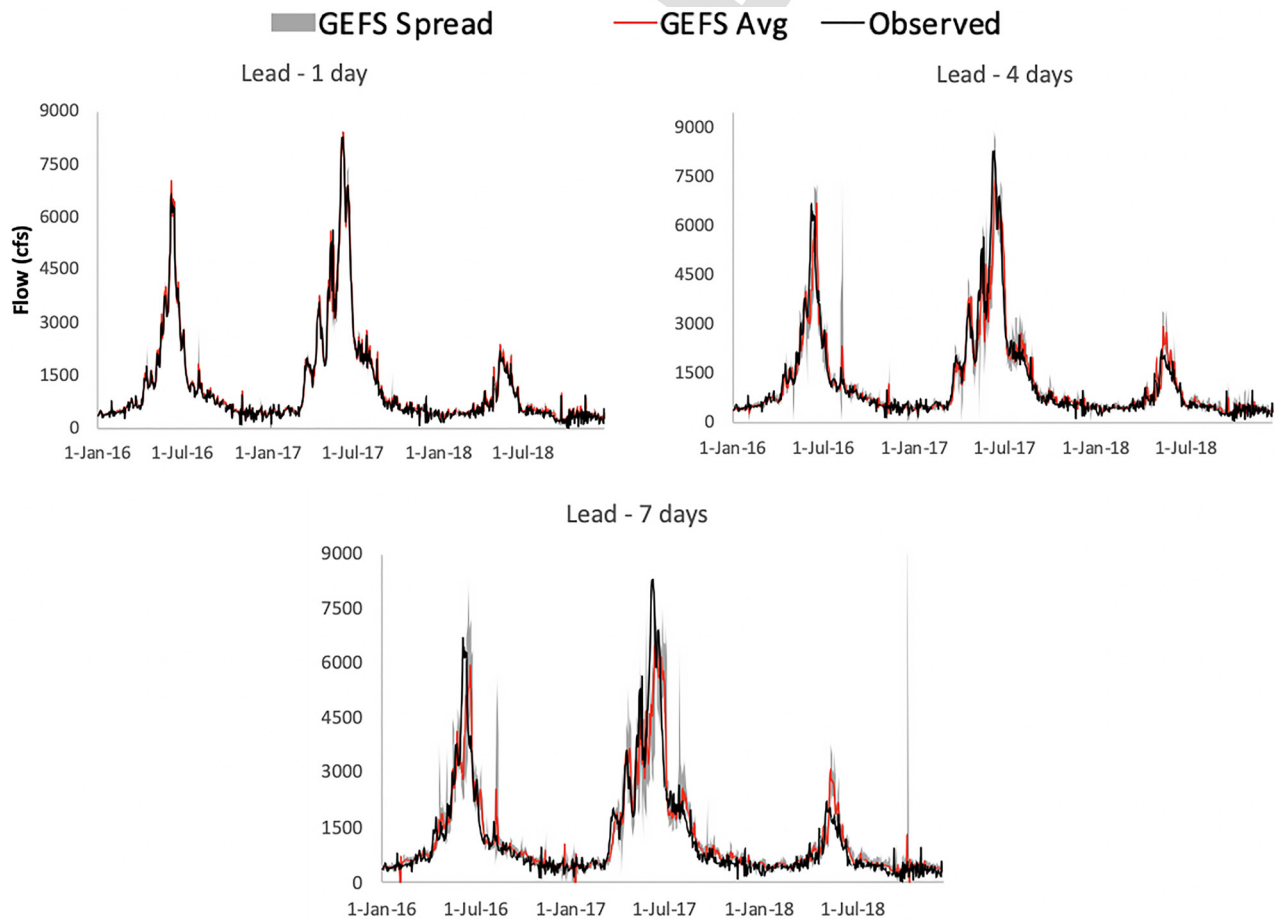
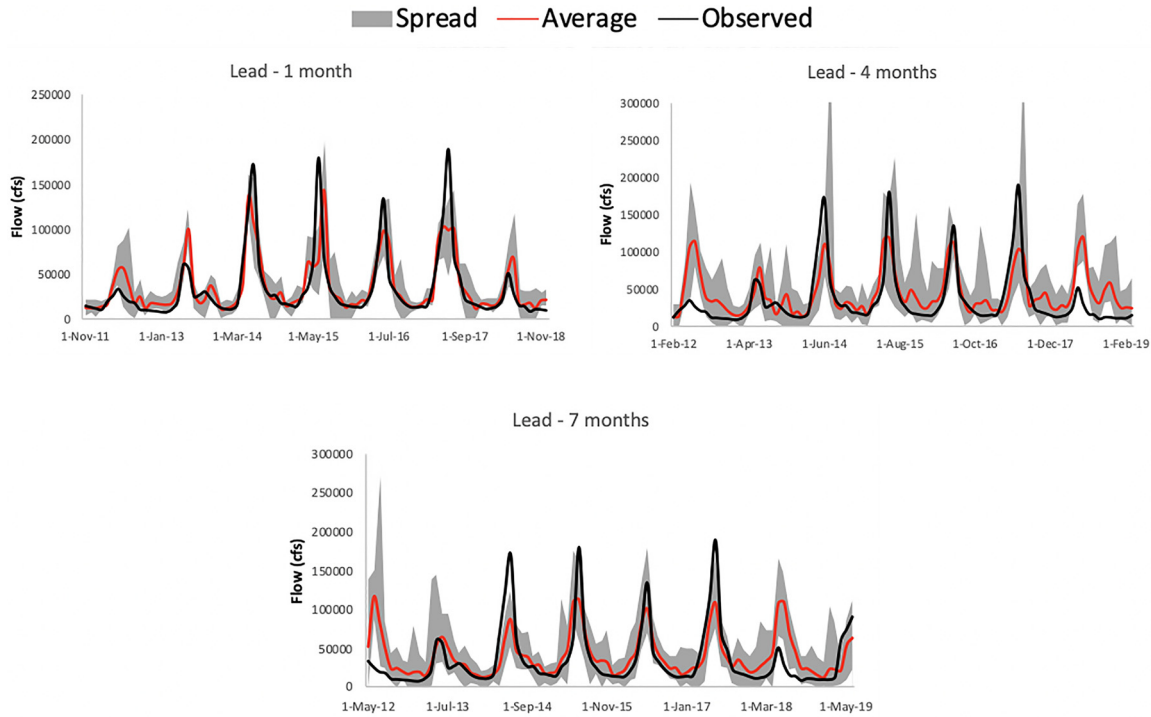
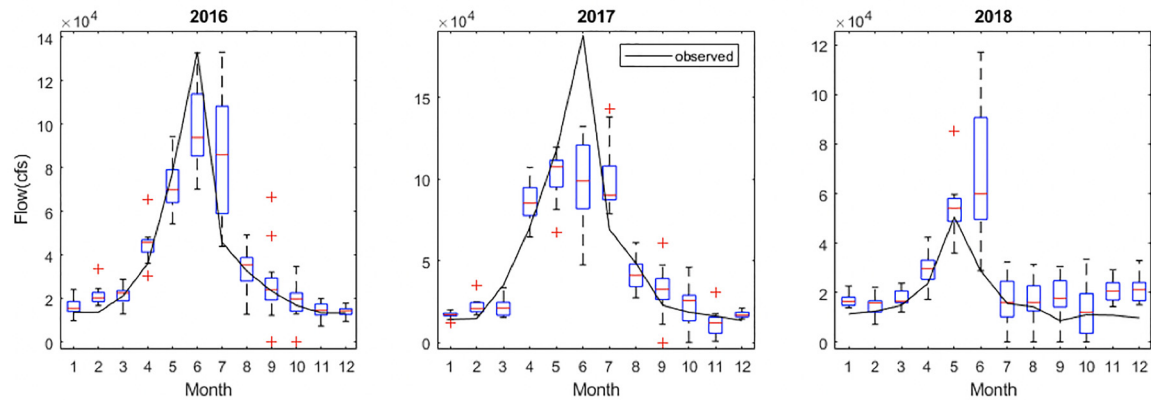


FIG. 11. Daily ensemble inflow forecasts along with the observed flow and average scenario of the 11-member ensemble for the Blue Mesa dam over 2016–2018.



(a)



(b)

FIG. 12. (a) Ensemble monthly flow forecasts using the ANN model compared against the observed inflows over the testing period for lead times of 1, 4, and 7 months; (b) box-plots of the ensemble flow forecasts for 2016–2018 showing the spread in the forecasts for the lead time of 1-month.

TABLE VIII. Evaluation metrics for assessing the performance of the average scenario from the ensemble of monthly flow forecasts over the testing period of the ANN model.

Metric	Lead 1 month	Lead 4 months	Lead 7 months
NSE	0.63	0.53	0.58
Correlation	0.80	0.75	0.77

2. Long-term inflow forecasts

913

The long-term ANN model was trained using the selected predictors, and ensemble forecast forcings were used to result in the ensemble of flow forecasts. The modeled monthly flow forecasts over the testing period are compared with the observed inflow in Fig. 12(a). The spread in the ensemble forecasts for the lead time of 1 month for Blue Mesa dam is shown as the box-plot in Fig. 12(b).

914

915

916

917

918

919

920 The average forecast scenario was used for performing the deter-
 921 ministic genetic algorithm-based optimization. The metrics evaluat-
 922 ing the performance of average monthly forecast scenario against
 923 the observed values are tabulated in Table VIII.

924 REFERENCES

925 Ahmad, S. K. and Hossain, F., "A generic data-driven technique for forecasting of
 926 reservoir inflow: Application for hydropower maximization," *Environ. Modell.*
 927 *Software* **119**, 147–165 (2019).
 928 Ahmad, S. K. and Hossain, F., "Maximizing energy production from hydropower
 929 dams using short-term weather forecasts," *Renewable Energy* **146**, 1560–1577
 930 (2020).
 931 Alemu, E. T., Palmer, R. N., Polebitski, A., and Meaker, B., "Decision support sys-
 932 tem for optimizing reservoir operations using ensemble streamflow pre-
 933 dictions," *J. Water Resour. Plann. Manage.* **137**(1), 72–82 (2011).
 934 Ancil, F., Perrin, C., and Andréassian, V., "Impact of the length of observed
 935 records on the performance of ANN and of conceptual parsimonious rainfall-
 936 runoff forecasting models," *Environ. Modell. Software* **19**, 357–368 (2004).
 937 Anghileri, D., Voisin, N., Castelletti, A., Pianosi, F., Nijssen, B., and Lettenmaier,
 938 D. P., "Value of long-term streamflow forecasts to reservoir operations for
 939 water supply in snow-dominated river catchments," *Water Resour. Res.* **52**,
 940 4209–4225, <https://doi.org/10.1002/2015WR017864> (2016).
 941 Archibald, T. W., McKinnon, K. I. M., and Thomas, L. C., "An aggregate stochas-
 942 tic dynamic programming model of multi-reservoir systems," *Water Resour.*
 943 *Res.* **33**(2), 333–340, <https://doi.org/10.1029/96WR02859> (1997).
 944 Aspinall Unit Water Operations, [https://www.usbr.gov/rsvrWater/
 945 HistoricalApp.html](https://www.usbr.gov/rsvrWater/HistoricalApp.html) for "Bureau of Reclamation" (2019); (accessed June 26, 2019).
 946 Becker, L., Yeh, W. W., Fults, D., and Sparks, D., "Operations models for cen-
 947 tral valley project," *J. Water Resour. Plann. Manage. Div.* **102**, 101–115
 948 (1976).
 949 Becker, L. and Yeh, W. W. G., "Optimization of real time operation of a multi-
 950 ple-reservoir system," *Water Resour. Res.* **10**(6), 1107–1112, [https://doi.org/
 951 10.1029/WR010i006p01107](https://doi.org/10.1029/WR010i006p01107) (1974).
 952 Block, P., "Tailoring seasonal climate forecasts for hydropower operations,"
 953 *Hydrol. Earth Syst. Sci.* **15**(4), 1355–1368 (2011).
 954 Celeste, A. B., Suzuki, K., and Kadota, A., "Integrating long- and short-term reser-
 955 voir operation models via stochastic and deterministic optimization: Case study
 956 in Japan," *J. Water Resour. Plann. Manage.* **134**(5), 440–448 (2008).
 957 Coulibaly, P., Ancil, F., and Bobée, B., "Daily reservoir inflow forecasting using
 958 artificial neural networks with stopped training approach," *J. Hydrol.* **230**,
 959 244–257 (2000).
 960 De Vos, N. J. and Rientjes, T. H. M., "Constraints of artificial neural networks for
 961 rainfall–runoff modelling: Trade-offs in hydrological state representation and
 962 model evaluation," *Hydrol. Earth Syst. Sci.* **9**(1/2), 111–126 (2005).
 963 Deb, K., Pratap, A., Agarwal, S., and Meyarivan, T., "A fast and elitist multiobjec-
 964 tive genetic algorithm: NSGA-II," *IEEE Trans. Evol. Comput.* **6**, 182–197
 965 (2002).
 966 Delworth, T. L., Broccoli, A. J., Rosati, A., Stouffer, R. J., Balaji, V., Beesley, J. A.,
 967 Cooke, W. F., Dixon, K. W., Dunne, J., Dunne, K. A., and Durachta, J. W.,
 968 "GFDL's CM2 global coupled climate models. Part I: Formulation and simula-
 969 tion characteristics," *J. Clim.* **19**(5), 643–674 (2006).
 970 DOE (U.S. Department of Energy), *Hydropower Vision: A New Chapter for*
 971 *America's 1st Renewable Electricity Source* (Department of Energy,
 972 Washington, DC, 2016).
 973 Dong, X., Dohmen-Janssen, C. M., Booij, M., and Hulscher, S., "Effect of flow
 974 forecasting quality on benefits of reservoir operation—A case study for the
 975 Geheyan reservoir (China)," *Hydrol. Earth Syst. Sci. Discuss.* **3**(6), 3771–3814
 976 (2006).
 977 Fan, F. M., Schwanenberg, D., Alvarado, R., Dos Reis, A. A., Collischonn, W.,
 978 and Naumann, S., "Performance of deterministic and probabilistic hydrologi-
 979 cal forecasts for the short-term optimization of a tropical hydropower reser-
 980 voir," *Water Resour. Manage.* **30**(10), 3609–3625 (2016).
 981 Fang, H. B., Hu, T. S., Zeng, X., and Wu, F. Y., "Simulation-optimization model
 982 of reservoir operation based on target storage curves," *Water Sci. Eng.* **7**(4),
 983 433–445 (2014).

Funk, C., Peterson, P., Landsfeld, M., Pedreros, D., Verdin, J., Shukla, S., Husak, 984
 G., Rowland, J., Harrison, L., Hoell, A., and Michaelsen, J., "The climate haz- 985
 ards infrared precipitation with stations—A new environmental record for 986
 monitoring extremes," *Sci. Data* **2**, 150066 (2015). 987
 Ge, X., Zhang, L., Shu, J., and Xu, N., "Short-term hydropower optimal schedul- 988
 ing considering the optimization of water time delay," *Electr. Power Syst. Res.* 989
110, 188–197 (2014). 990
 Georgakakos, A. P., *Decision Support Systems for Water Resources Management: 991*
Nile Basin Applications and Further Needs (■, Atlanta, GA, 2006), pp. 1–22. 992
 Georgakakos, K., Graham, N., Carpenter, T., and Yao, H., "Integrating climate- 993
 hydrology forecasts and multi-objective reservoir management for Northern 994
 California," *EOS Trans. Am. Geophys. Union* **86**(12), 122–127 (2005). 995
 Golembesky, K., Sankarasubramanian, A., and Devineni, N., "Improved drought 996
 management of Falls Lake Reservoir: Role of multimodel streamflow forecasts 997
 in setting up restrictions," *J. Water Resour. Plann. Manage.* **135**(3), 188–197 998
 (2009). 999
 Hamill, T. M., Bates, G. T., Whitaker, J. S., Murray, D. R., Fiorino, M., Galarneau, 1000
 Jr., T. J., Zhu, Y., and Lapenta, W., "NOAA's second-generation global 1001
 medium-range ensemble reforecast data set," *Bull. Am. Meteorol. Soc.* **94**, 1002
 1553–1565 (2013). 1003
 Hamlet, A. F., Huppert, D., and Lettenmaier, D. P., "Economic value of long-lead 1004
 streamflow forecasts for Columbia River hydropower," *J. Water Resour. Plann.* 1005
Manage. **128**(2), 91–101 (2002). 1006
 Holmes, K. J. and Papay, L., "Prospects for electricity from renewable resources 1007
 in the United States," *J. Renewable Sustainable Energy* **3**(4), 042701 (2011). 1008
 Kirtman, B. P., Min, D., Infanti, J. M., Kinter III, J. L., Paolino, D. A., Zhang, Q., 1009
 Van Den Dool, H., Saha, S., Mendez, M. P., Becker, E., and Peng, P., "The 1010
 North American multimodel ensemble: Phase-1 seasonal-to-interannual pre- 1011
 diction; phase-2 toward developing intraseasonal prediction," *Bull. Am.* 1012
Meteorol. Soc. **95**(4), 585–601 (2014). 1013
 Li, Q., Yu, M., Zhao, J., Cai, T., Lu, G., Xie, W., and Bai, X., "Impact of the three 1014
 Gorges reservoir operation on downstream ecological water requirements," 1015
Hydrol. Res. **43**(1–2), 48–53 (2012). 1016
 Ligon, F. K., Dietrich, W. E., and Trush, W. J., "Downstream ecological effects of 1017
 dams," *BioScience* **45**(3), 183–192 (1995). 1018
 Liu, H., "On the Levenberg-Marquardt training method for feed-forward neural 1019
 networks," in *Proceedings of 6th International Conference on Natural* 1020
Computation (2010), Vol. 1, pp. 456–460. 1021
 Liu, P., Guo, S., Xu, X., and Chen, J., "Derivation of aggregation-based joint oper- 1022
 ating rule curves for cascade hydropower reservoirs," *Water Resour. Manage.* 1023
25(13), 3177–3200 (2011). 1024
 Lund, J. R. and Guzman, J., "Derived operating rules for reservoirs in series or in 1025
 parallel," *J. Water Resour. Plann. Manage.* **125**(3), 143–153 (1999). 1026
 Madsen, H., Richaud, B., Pedersen, C. B., and Borden, C., "A real-time inflow 1027
 forecasting and reservoir optimization system for optimizing hydropower 1028
 production," in *Waterpower XVI* (2009), Vol. 1, p. 12. 1029
 Manyari, W. V. and de Carvalho, Jr., O. A., "Environmental considerations in 1030
 energy planning for the Amazon region: Downstream effects of dams," *Energy* 1031
Policy **35**(12), 6526–6534 (2007). 1032
 Marques, G. F. and Tilmant, A., "The economic value of coordination in large- 1033
 scale multireservoir systems: The Parana River case," *Water Resour. Res.* **49**, 1034
 7546–7557, <https://doi.org/10.1002/2013WR013679> (2013). 1035
 Maurer, E. P. and Lettenmaier, D. P., "Potential effects of long-lead hydrologic 1036
 predictability on Missouri River main-stem reservoirs," *J. Clim.* **17**(1), 174–186 1037
 (2004). 1038
 Montanari, A. and Grossi, G., "Estimating the uncertainty of hydrological fore- 1039
 casts: A statistical approach," *Water Resour. Res.* **44**(12), ■ (2008). 1040
 Monteiro, C., Ramirez-Rosado, I. J., and Fernandez-Jimenez, L. A., "Short-term 1041
 forecasting model for electric power production of small-hydro power plants," 1042
Renewable Energy **50**, 387–394 (2013). 1043
 Quinn, J. D., Reed, P. M., Giuliani, M., and Castelletti, A., "What is controlling 1044
 our control rules? Opening the black box of multi-reservoir operating policies 1045
 using time-varying sensitivity analysis," *Water Resour. Res.* **55**, 5962–5984, 1046
<https://doi.org/10.1029/2018WR024177> (2019). 1047
 Raso, L., Schwanenberg, D., van de Giesen, N. C., and van Overloop, P. J., "Short- 1048
 term optimal operation of water systems using ensemble forecasts," *Adv.* 1049
Water Resour. **71**, 200–208 (2014). 1050

AQ7

AQ8

AQ10

AQ11

- 1051 Saad, M., Turgeon, A., Bigras, P., and Duquette, R., "Learning disaggregation
1052 technique for the operation of long-term hydroelectric power systems,"
1053 *Water Resour. Res.* **30**(11), 3195–3202, <https://doi.org/10.1029/94WR01731>
1054 (1994).
- 1055 Saha, S., Moorthi, S., Wu, X., Wang, J., Nadiga, S., Tripp, P., Behringer, D., Hou,
1056 Y. T., Chuang, H. Y., Iredell, M., and Ek, M., "The NCEP climate forecast sys-
1057 tem version 2," *J. Clim.* **27**(6), 2185–2208 (2014).
- 1058 Sankarasubramanian, A., Lall, U., Devineni, N., and Espinueva, S., "The role of
1059 monthly updated climate forecasts in improving intraseasonal water
1060 allocation," *J. Appl. Meteorol. Climatol.* **48**(7), 1464–1482 (2009).
- 1061 Sikder, S. and Hossain, F., "Assessment of the weather research and forecasting
1062 model generalized parameterization schemes for advancement of precipitation
1063 forecasting in monsoon-driven river basins," *J. Adv. Model. Earth Syst.* **8**, 1210
1064 (2016).
- 1065 Souza, T. M. and Diniz, A. L., "An accurate representation of water delay times
1066 for cascaded reservoirs in hydro scheduling problems," in *IEEE Power and*
1067 *Energy Society General Meeting* (IEEE, 2012).
- 1068 Sreekanth, J., Datta, B., and Mohapatra, P. K., "Optimal short-term reservoir
1069 operation with integrated long-term goals," *Water Resour. Manage.* **26**(10),
1070 2833–2850 (2012).
- 1071 Sudheer, K. P., Nayak, P. C., and Ramasatri, K. S., "Improving peak flow esti-
1072 mates in artificial neural network river flow models," *Hydrol. Processes* **17**,
1073 677–686 (2003).
- 1074 Tilt, B., Braun, Y., and He, D., "Social impacts of large dam projects: A compari-
1075 son of international case studies and implications for best practice," *J. Environ.*
1076 *Manage.* **90**, S249–S257 (2009).
- 1077 Turner, S. W., Bennett, J. C., Robertson, D. E., and Galelli, S., "Complex relation-
1078 ship between seasonal streamflow forecast skill and value in reservoir oper-
1079 ations," *Hydrol. Earth Syst. Sci.* **21**(9), 4841–4859 (2017).
- Turner, S. W. D. and Galelli, S., "Water supply sensitivity to cli-
1080 mate change: An R package for implementing reservoir storage analysis in global and regional
1081 impact studies," *Environ. Modell. Software* **76**, 13–19 (2016).
- 1082 USBR (U.S. Bureau of Reclamation), *Aspinall Unit Operations Final*
1083 *Environmental Impact Statement-Background Material* (Bureau of
1084 Reclamation, Utah, 2004).
- 1085 USBR (U.S. Bureau of Reclamation), *Aspinall Unit Operations Final*
1086 *Environmental Impact Statement* (Bureau of Reclamation, Utah, 2012a).
- 1087 USBR (U.S. Bureau of Reclamation), *Record of Decision for the Aspinall Unit*
1088 *Operations Final Environmental Impact Statement* (Bureau of Reclamation,
1089 Utah, 2012b).
- 1090 Xu, B., Zhong, P.-A., Stanko, Z., Zhao, Y., and Yeh, W. W.-G., "A multiobjective
1091 short-term optimal operation model for a cascade system of reservoirs consid-
1092 ering the impact on long-term energy production," *Water Resour. Res.* **51**,
1093 3353–3369, <https://doi.org/10.1002/2014WR015964> (2015).
- 1094 Yang, T., Asanjan, A. A., Welles, E., Gao, X., Sorooshian, S., and Liu, X.,
1095 "Developing reservoir monthly inflow forecasts using artificial intelligence and
1096 climate phenomenon information," *Water Resour. Res.* **53**, 2786–2812, [https://](https://doi.org/10.1002/2017WR020482)
1097 doi.org/10.1002/2017WR020482 (2017).
- 1098 Yeh, W. W. G., "Real-time reservoir operation: The California central valley proj-
1099 ect case study," paper presented at the National Workshop on Reservoir
1100 Systems Operations, American Society of Civil Engineers (ASCE), Boulder,
1101 Colorado, 1979.
- 1102 Zealand, C. M., Burn, D. H., and Simonovic, S. P., "Short term streamflow fore-
1103 casting using artificial neural networks," *J. Hydrol.* **214**(1-4), 32–48 (1999).
- 1104 Zhang, G., Patuwo, B. E., and Hu, M. Y., "Forecasting with artificial neural net-
1105 works: The state of the art," *Int. J. Forecasting* **14**, 35–62 (1998).
- 1106 Zhou, Y., Guo, S., Liu, P., Xu, C. Y., and Zhao, X., "Derivation of water and power
1107 operating rules for multi-reservoirs," *Hydrol. Sci. J.* **61**(2), 359–370 (2016).
- 1108